Invited review

The distribution of rivers to terrestrial sinks: Implications for sediment routing systems

Björn Nyberg *, Robert L. Gawthorpe, William Helland-Hansen

Department of Earth Sciences, University of Bergen, P.O. Box 7803, 5020 Bergen, Norway

A B S T R A C T

Empirical observations used to constrain controls on large global modern river systems typically use catchment delineations depicting drainage patterns of rivers to oceans. A key component in the spatial and temporal discharge of sediment to oceans are terrestrial sinks that act as buffers and sequestrate sediment and nutrients along its route, however, a global catchment model depicting the drainage patterns of rivers to terrestrial sinks does not currently exist. We propose a new global terrestrial sink catchment (GTSC) database that delineates the distribution of high-resolution global river networks in relation to mapped modern terrestrial sinks.

The results show a distinct set of characteristics defining the morphology, climate, lithology and sediment discharge of source catchments contributing to terrestrial sinks by tectonic regime. Foreland, intracratonic, extensional and strike-slip tectonic regimes are characterized by small, numerous, densely spaced and wide source catchments where the largest source catchment contributes on average 50%, 43%, 36% and 36%, respectively, of the total suspended sediment load. Forearc and passive margin tectonic regimes are characterized by few, large source catchments where the largest source catchment contributes on average 64% and 63% of the total suspended sediment load. In contrast to forearc and passive margin settings, foreland, intracratonic, extensional and strike-slip settings show source catchments with a range of lithologies and a dominance of seasonal climates, which will likely increase along-strike variability in sediment discharge to their terrestrial sink.

The variability of along-strike sediment discharge, sediment composition and source-derived perturbations in sediment discharge to the terrestrial sink will influence the sediments stored and propagation of sediment discharge signals. On geological timescales, marine sedimentary successions and the sediment routing system, likely represents the characteristics of remobilized terrestrial sink sediments during millennial scale perturbations in water discharge. The GTSC database provides a valuable resource to further our quantitative understanding on the role of the terrestrial sink on the broader sediment routing system.

Contents

* Corresponding author.
  E-mail address: bjorn.nyberg@uib.no (B. Nyberg).

1. Introduction

Rivers and their drainage patterns on continental land masses play a vital role in the hydrological cycle. The hydrological drainage pattern, known as catchments, distribute water, organize sediment and transport nutrients from source to endorheic (internal) or exorheic (coastal) sinks. This has wide ranging implications for shaping landscapes, mountain building processes, water-atmosphere interactions, biogeochemical cycles, ecological and biological influences, water resources and socio-economic concerns (Vörösmarty et al., 2000a; Syvitski et al., 2005; Laruelle et al., 2013; Bierkens, 2015). In the past two decades, catchment models depicting hydrological drainage systems have shifted from isolated regional scale studies to a global and quantitative perspective to improve the complete closed-system analysis of the cycle (Vörösmarty et al., 2000a).

From a geomorphological and sedimentological perspective, the catchment defines the sediment routing system from source, transport and deposition of siliclastic material, otherwise known as the source-to-sink system (for a comprehensive review, see Helland-Hansen et al., 2016). The terrestrial sink or modern terrestrial sedimentary basin represents areas of Earth's surface that are undergoing subsidence and creating accommodation space for potential sediment preservation (Jervey, 1988; Blum and Tornqvist, 2000; Romans et al., 2016). Given that the sedimentary rock record is a history of only the preserved depositional record (Miall, 2014), distinguishing modern terrestrial sinks from their erosional counterpart, and understanding the spatial and temporal coupling between the two, is an important factor in applying geomorphological observations of the present to the past (Davidson et al., 2013; Helland-Hansen et al., 2016).

Recently, Nyberg and Howell (2015) aerially described the global terrestrial distribution of modern sedimentary basins as including 16% of the continental land surface. These modern terrestrial sedimentary basins (or terrestrial sinks) have in recent years been the focus of high-resolution and freely accessible remotely sensed imagery studies through products such as Google Earth, allowing a revitalization of global and quantitative modern geomorphological research. For instance, Hartley et al. (2010) and Weissmann et al. (2010) have documented that fluvial systems within the bounds of modern terrestrial sinks are dominated by a distinct distributive fluvial characteristics that have important paleogeographical implications for ancient sedimentary successions (Davidson et al., 2013). Despite the importance of the terrestrial sink on our geomorphological understanding of the sedimentary record, its relation to the global drainage pattern of rivers has previously not been established.

Vorosmarty et al. (2000a) constructed a global digitized topological river network representing drainage patterns of the non-glaciated continental landmass highlighting stream order contributions to the oceans at a 30-arc minute resolution. Their classification subdivided catchments based on continents, endorheic and exorheic drainage basins and quantified geometric attributes of river segment order, river length and catchment area. The river network delineation of Vörösmarty et al. (2000a) has played a pivotal role in numerous hydrological water balance, sediment budget models and land-atmosphere studies (Vörösmarty et al., 2000b; Syvitski et al., 2005; Syvitski and Milliman, 2007; Wisser et al., 2010; Dürr et al., 2011). Döll and Lehner (2002) suggested a new global 30-arc minute drainage direction map for the delineation of catchments, and more recently HydroSHEDS (Lehner et al., 2008) provides high-resolution catchments based on improved digital elevation models (DEM) at 3-arc second resolution within ±60° latitude. In addition, procedures to delineate river networks and drainage catchments have continuously improved to derive more reliable hydrological models (e.g., Wisser et al., 2010; Getirana et al., 2012; Bierkens, 2015). However, none of the global based catchment models mentioned above delineates the distribution of rivers to terrestrial sinks.

The aim of this paper is to introduce a new digital catchment database depicting the drainage patterns of rivers to global terrestrial sinks. We describe the methodology and summarize the global tectonic, climatic, geometrical and lithological distributions of the global terrestrial sink catchment (GTSC) database. Finally, we discuss the implications of the results on sediment signal propagation to the terrestrial sink and its influence on the broader sediment routing system on geological timescales.

2. Methodology

Here we present the data sources and methodology used to derive the global terrestrial sink catchment (GTSC) database. The global-based catchment database defines the drainage patterns to exorheic (Fig. 1A) and endorheic sinks (Fig. 1C). In this study, we considered an exorheic catchment as the drainage area of rivers to a coastal body of water including the alluvial fan and its axial fluvial component. An endorheic catchment was defined as the drainage area of a river to an internal sink (i.e., no coastal outlet). Subsequently, sub-catchments were defined within each exorheic/endorheic catchment (Fig. 1B and D) to represent the distribution of rivers in relation to modern terrestrial sinks (Fig. 2).

Terrestrial sinks, otherwise known as terrestrial sedimentary basins, reflect a low-lying region that has undergone subsidence and created accommodation space for sediment accumulation during the Quaternary (Nyberg and Howell, 2015). The region represents modern
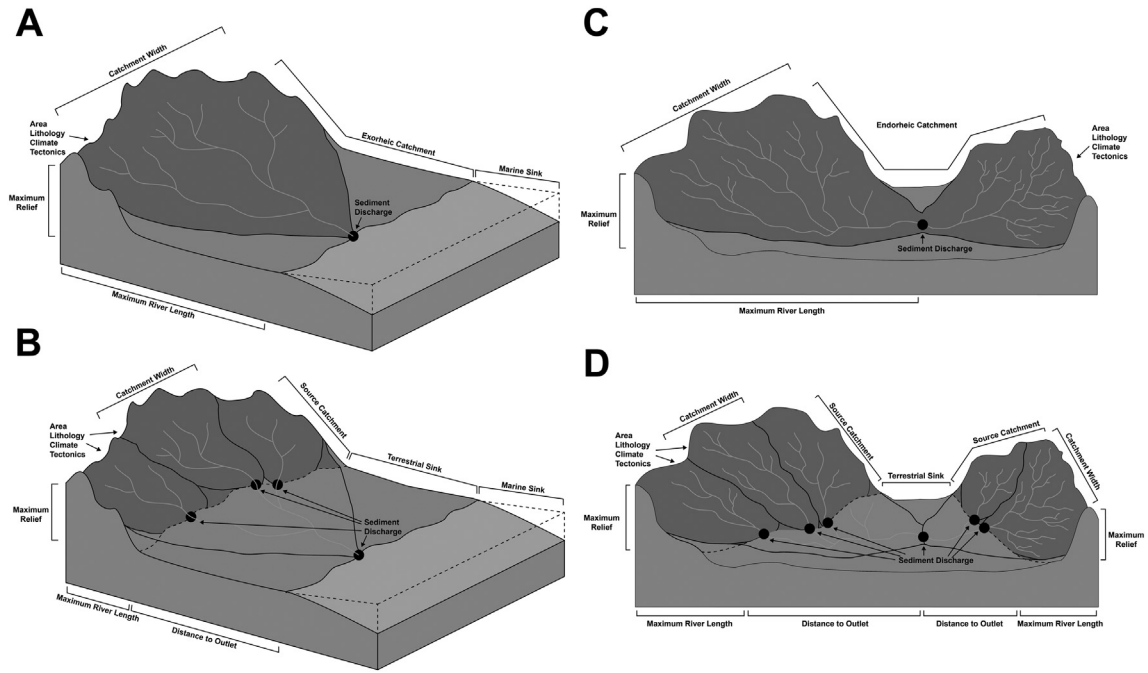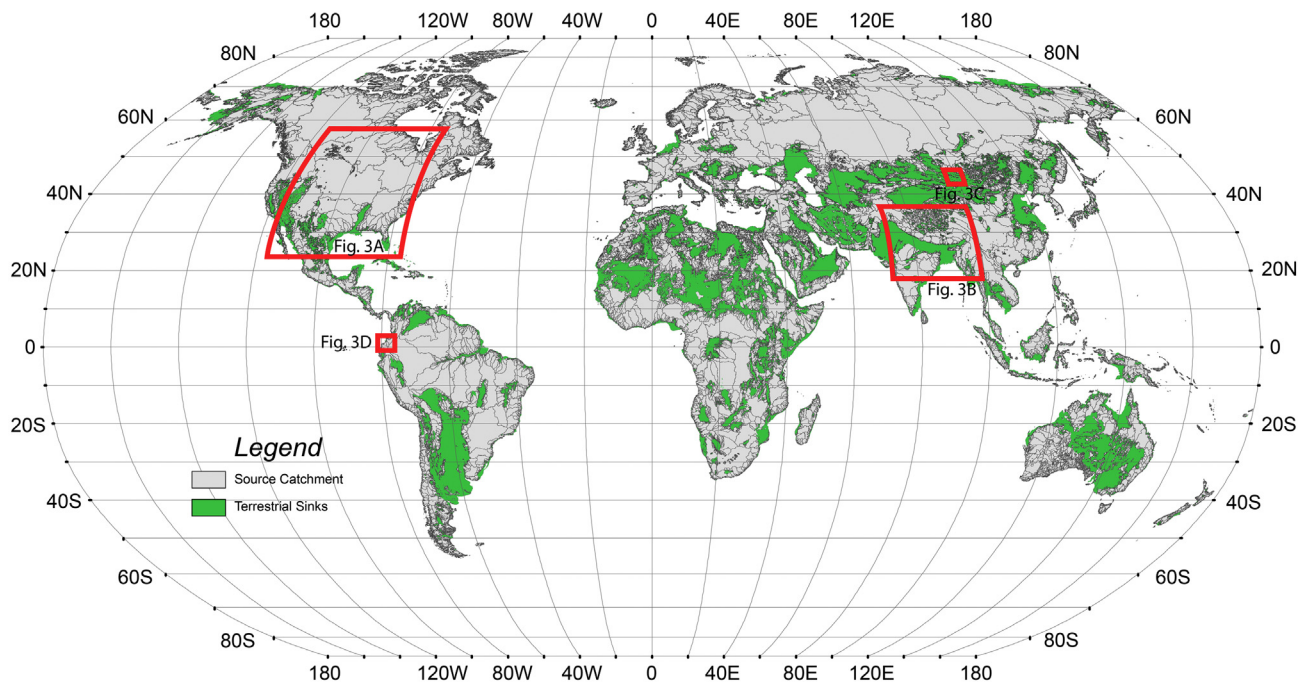
Fig. 1. Delineation of terrestrial sink catchments. (A) shows the delineation of an exorheic catchment by calculating the cumulative upstream contribution from its marine sink. (B) shows sub-catchments within the larger exorheic catchment representing the cumulative upstream contribution from each locality where the river network drains into the terrestrial sink. (C) shows the delineation of an endorheic catchment by calculating the cumulative upstream contribution from an internal drainage river network. (D) shows sub-catchments within the larger endorheic catchment representing the cumulative upstream contribution from each locality where the river network drains into the terrestrial sink. River length, relief, width, sediment discharge, area, lithology, climate and tectonics are identified for each catchment or source catchment.

terrestrial sedimentary basins with long-term (>10^6 yr) sediment ag-gradation including both alluvial fan and fluvial components that have preservation potential. This excludes, for example, large portions of the Canadian Shield and Siberian Platform that are in present-day iso-static rebound since the last glacial maximum. Exorheic catchments (i.e., externally draining systems) may or may not include a terrestrial sink region if the river drains through a terrestrial sedimentary

basin (e.g., Figs. 1A–B, 3A–C). Endorheic catchments (i.e., internally draining systems) often terminate in the region of a terrestrial sink (e.g., Figs. 1D and 3D) but also include short-lived endorheic catchments without long-term terrestrial sink preservation.

Geometric attributes, lithology, total suspended sediment discharge, tectonic regime and climate were classified for each catchment and sub-catchment region (Fig. 1). It is important to note that the current

Fig. 2. Global distribution of rivers to terrestrial sinks. The map shows the Global Terrestrial Sink Catchment (GTSC) database depicting rivers contributing to terrestrial sinks as defined by Nyberg and Howell (2015). The map is shown with a Robinson projection.
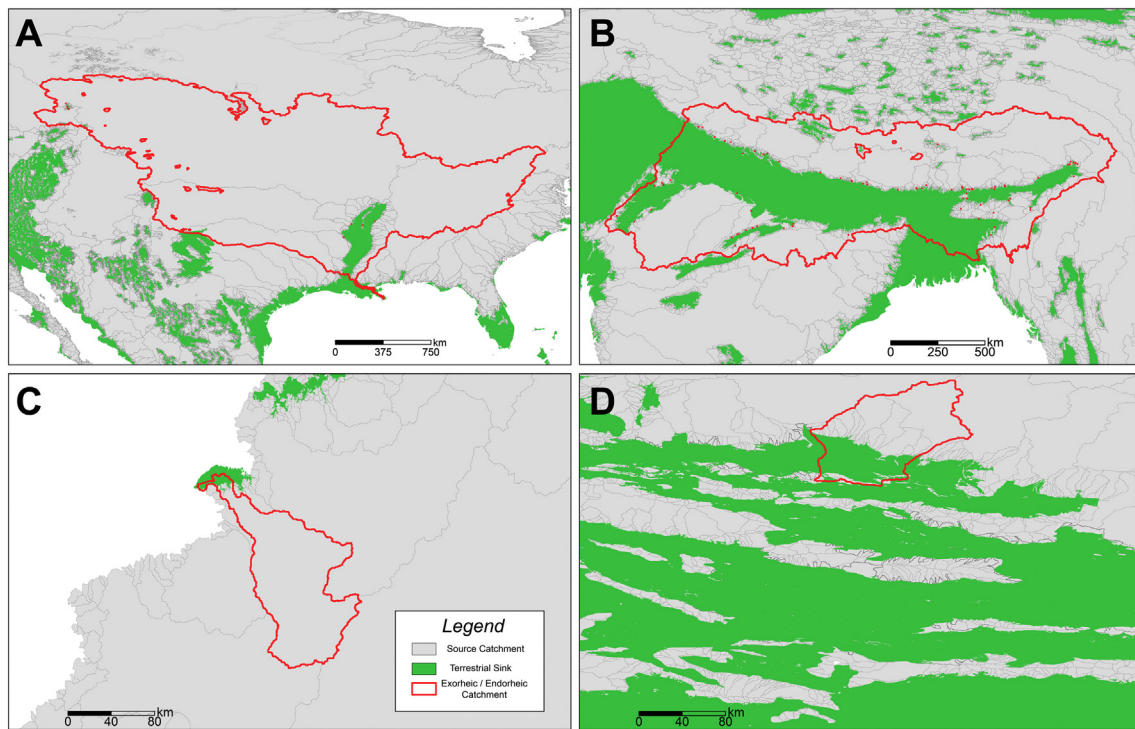
Fig. 3. Examples of the Global Terrestrial Sink Catchment (GTSC) database. The figure shows the contributing source catchments to the terrestrial sink for (A) the exorheic passive margin Mississippi catchment; (B) the exorheic foreland Ganges/Brahmaputra catchment; (C) the exorheic forearc Andean catchment and (D) the endorheic strike-slip/extensional Mongolian catchments. See Fig. 2 for location. Maps are a Cylindrical Equal Area projection.

database does not consider any hydrological groundwater connection or the larger drainage basin area that may merge during flood episodes or sea-level fluctuations.

2.1. Global catchments

To define global catchments, a consistent hydrologically conditioned digital elevation model (DEM) was created. HydroSHEDS provides a globally conditioned DEM between 60°N and 60°S at a 15-arc second resolution based on SRTM data. SRTM v 4.1 DEM has a vertical resolution accuracy within <16 m (Reuter et al., 2007; Lehner et al., 2008). While a higher resolution 3-arc second SRTM DEM product exists, the chosen resolution reflects the resolution available for DEMs at higher latitudes (>60°N). To supplement the dataset, a 15-arc second breakline emphasis GMTED2010 was used between 40°N and 90°N that is based on a resampled method preserving drainage ridges. A 20° overlap ensures a complete coverage of catchment drainage patterns to Arctic coastlines. GMTED2010 has root mean squared vertical error of −1.01 m (±31.24 m; Danielson and Gesch, 2011). Antarctica and Greenland were excluded from the analyses given that these areas are predominately ice-covered, which is also consistent with the coverage of global terrestrial sedimentary basins used in this study (Nyberg and Howell, 2015). The GMTED2010 DEM was conditioned by removing small internally draining sinks and/or barriers that are within 10 m along the drainage profile.

The flow direction was calculated for each DEM model by measuring elevation change within a 3 by 3 matrix window. The flow direction can subsequently be used to calculate the cumulative upstream contributing area for each grid cell as a flow accumulation parameter. These are standard geographical information system (GIS) tools that were executed within ArcGIS (ESRI, 2017). A cumulative 250 grid cell flow accumulation was used as a threshold to define a global rasterized river network. For each set of river networks, the corresponding flow accumulation raster was extracted and analyzed for its highest cumulative

flow component. This highest flow accumulation grid cell within each river network cluster defined its sink. This ensured that the sink was properly identified, even in endorheic catchments where its sink locality can occur along a river segment (e.g., Fig. 1C). The resulting product was a global coverage of endorheic and exorheic sinks.

The area upstream of the sink defined the catchment area (Fig. 1) as vectorized polygons. Finally, overlap between the two datasets were handled by removing area from the GMTED2010 catchment delineations using the higher DEM resolution and accuracy of the SRTM catchment delineations. A global river network product was subsequently merged based on the relevant DEM model that was used in its global catchment delineation.

2.2. Terrestrial sink catchments

The entry and exit localities of the global river network as it flows into and out of the terrestrial sink area defined by Nyberg and Howell (2015) was achieved by intersecting the two products to create a set of coordinates. This highlightd both the drainage patterns to, as well as the internal drainage patterns of, the terrestrial sink region (e.g., Fig. 1). Duplicate sink coordinates in the terrestrial sink dataset were removed that were consistent with the exorheic/endorheic sink dataset. The terrestrial, exorheic and endorheic sinks define a global dataset of sinks. The resulting information of sink localities was used to define upstream area of each sink to define a global database of terrestrial sink catchments (Fig. 2).

Given the large volume of data, sub-catchments were analyzed in sections based on the global catchment delineation and implemented into a multiprocessing workflow within the Python programming language. This process sectioned catchments on the global scale into their individual flow direction, flow accumulation, river network and sink localities components. This significantly improved the feasibility to process the numerous sub-catchments that may occur within a larger catchment region in relation to the global terrestrial sinks.

2.3. Endorheic vs. exorheic catchments

Distinguishing endorheic vs. exorheic catchments was handled by assigning catchment sinks within 10 km of the shoreline as exorheic, otherwise they were considered as endorheic catchments. This threshold was chosen because a river network may terminate early on the floodplain due to the inadequate representation of flow direction by the DEM delineation. The shoreline definition included the Black Sea but excluded land-locked water bodies including the Caspian Sea and Aral Sea. The resulting characterization was manually analyzed by examining the classification and its catchment sink in relation to global based imagery to include catchment definitions where a visible coastal connection was apparent or removed where a visible coastal connection was not apparent.

Exorheic catchments were furthermore characterized based on epicontinental seaways or non-epicontinental seaways on narrow (<75 km) and wide (>75 km) continental shelves based on the classification scheme of Nyberg and Howell (2016).

2.4. Geometric attributes

Geometric attributes of length, width, relief, area and minimum bounding box width and length were attributed to each catchment and sub-catchment region. Sub-catchments also recorded distance from an endorheic/exorheic sink. The length of each catchment, sub-catchment and distance to an endorheic/exorheic sink was achieved by segmenting the global river network at each vertex and at each terrestrial sink and treating each segmented river line as a series of start to end coordinates within a graph network. By assigning each coordinate pair a segment length and cumulatively measuring the distance from each endorheic or exorheic coordinate sink, a distance along the river network was obtained using a modified algorithm of Nyberg et al. (2015). The cumulative river network distance was used to derive catchment length, sub-catchment length and sub-catchment distance from the endorheic/exorheic sink.

Due to the irregularity of catchment shape, measuring width was a problematic and challenging issue. In the current study, the width of each catchment was determined as twice the maximum distance of the river segment distance from its catchment boundary. Relief of the catchment/sub-catchment was defined as its maximum range as measured from GMTED2010 global digital elevation data. The area of each catchment and source catchment region was defined by a global cylindrical equal area projection coordinate system.

2.5. Discharge

Defining the sediment load of the entire catchment system may be estimated using the BQART formula (Eq. (1)) as proposed by Syvitski and Milliman (2007), which explains 96% of 30-yr sediment load variation in modern rivers:

$$Qs = 0.0006(1 + 0.09Ag)L(1 - Te)EhQ^{0.31}A^{0.5}RT \ for \ T \geq 2\ ^{\circ}C \qquad (1a)$$

$$Qs = 0.0012(1 + 0.09Ag)L(1 - Te)EhQ^{0.31}A^{0.5}R \ for \ T < 2\ ^{\circ}C \qquad (1b)$$

where Qs is sediment load (MT/yr), Ag is the glacial coverage of the catchment as a percentage (0–100%), L is the lithology coefficient between 0.5 and 3, Te is the trapping efficiency as a percentage (0–100%), Eh is the anthropogenic influence that ranges from 0.3 to 2, Q is catchment discharge (km^3/yr), A is catchment area (km^2), R is maximum relief (km) and T is the mean basin temperature (°C). The catchment discharge (Q) was determined by:

$$Q = 0.075A^{0.8} \qquad (2)$$

The glacial coverage (Ag) of each catchment was accounted for by measuring the lithology distribution as defined by the global lithological

map database (GLiM; Hartmann and Moosdorf, 2012). The overall catchment lithology (L) and anthropogenic influence (Eh) has been based on the original global maps of Syvitski and Milliman (2007). The trapping efficiency (Te) of the major global catchments was defined based on the work by Vörösmarty et al. (2003). Relief (R) was taken by sampling the 99th percentile range within each catchment based on global GMTED2010 DEM coverage at a 15-arc second resolution (Danielson and Gesch, 2011). An averaged compiled dataset of daytime land surface temperature of 2013 based on the MODIS satellite (NASA LP DAAC, 2001) was used to define the mean catchment temperature (T).

Sediment discharge of source catchments to the terrestrial sinks was similarly calculated based on Eq. (1) (Fig. 1B, D) and subsequently adjusted based on its relative sediment load to the entire catchment region (Fig. 1A, C).

2.6. Tectonic regime

Three tectonic classifications are provided in the GTSC database. The first classification categorizes each internal sub-catchment according to the tectonic regime of the modern terrestrial sink classification as defined by Nyberg and Howell (2015), which represents six main tectonic regimes (Ingersoll, 2012): foreland, passive margin, intracratonic, forearc, extensional or strike-slip. The geographical distribution of these tectonic regimes is derived from published regional and global scale stress-maps, neotectonic maps, plate tectonic boundaries and previous tectonic basin classifications (e.g., Mann and Burke, 1984; Dewey et al., 1986; Watson et al., 1987; Müller et al., 1992; Zoback, 1992; Marsaglia, 1995; Decelles and Giles, 1996; Allmendinger et al., 1997; Honthaas et al., 1998; Bird, 2003; Yi et al., 2003; Yueqiao et al., 2003; Wang et al., 2006; Cunningham, 2010; Hartley et al., 2010; DeCelles et al., 2011; Ingersoll, 2012). The second tectonic regime classification reflects the main tectonic regime of exorheic catchments as it drains to the shoreline based on the work of Nyberg and Howell (2016). Lastly, a combined tectonic classification was used that employs the tectonic regime classification of the terrestrial sinks and the global exorheic tectonic regime classification to create a seamless tectonic classification scheme of both endorheic and exorheic catchments.

Each catchment was categorized based on either an active or passive shoreline margin, which reflects a common categorical scheme used in global geomorphological studies (Sømme et al., 2009; Harris et al., 2014) to separate mixed tectonically influenced systems. For instance, the Ganges/Brahmaputra represents a foreland tectonic regime but its delta and shoreline is on a predominately passive margin. In contrast, a majority of the catchments draining to the Red Sea are passive margins that occur at the active margin of the Red Sea rift (Harris et al., 2014).

2.7. Climate

Climate of the catchments was derived based on the Köppen-Geiger classification scheme (Kottek, 2006) that classifies climate regions by the seasonality of precipitation and temperature as captured by vegetation. The classification defines climate by a first order equatorial, arid, warm temperate, snow or polar scheme, followed by a second order precipitation and third order temperature classification (Table 1). Its implementation within the current dataset was handled by assigning two classifications based on the largest aerial coverage of the first order and second order classifications. In addition, the proportion of aerial overlap of each third order climate classification (e.g., AWh) within each catchment was recorded as a percentage (0–100%).

2.8. Lithological distribution

Catchment lithology plays an important role in denudation rates (Palumbo et al., 2009) and thereby an important control on sediment

Table 1
A summary of first- and second-order climate distributions by percentage area for each tectonic regime in the GTSC database.

Climate		Tectonics						
First-order climate	Second-order climate	Extensional	Fore-arc	Foreland	Intra-cratonic	Passive margin	Strike-slip	Subtotal
Equatorial (A)	Humid (f)	0.05	0.58	1.71	0.36	2.13	0.02	4.85
	Monsoon (m)	0.06	0.09	0.93	0.54	2.14	0.00	3.77
	Dry Summer (s)	0.04	0.03	0.01	0.05	0.40	0.02	0.56
	Dry Winter (w)	0.79	0.34	1.29	5.28	5.23	0.07	12.99
	Subtotal	0.94	1.04	3.94	6.24	9.89	0.11	22.16
Arid (B)	Dry Summer (s)	1.10	0.14	2.22	4.77	3.47	0.87	12.58
	Dry Winter (w)	0.42	0.26	2.87	11.33	2.71	0.92	18.50
	Subtotal	1.53	0.40	5.09	16.10	6.18	1.79	31.09
Warm Temperate (C)	Humid (f)	0.20	0.37	2.55	2.27	3.33	0.10	8.80
	Dry Summer (s)	0.34	0.39	1.15	0.15	0.53	0.29	2.85
	Dry Winter (w)	0.50	0.08	2.38	0.74	0.61	0.09	4.41
	Subtotal	1.04	0.84	6.08	3.16	4.47	0.47	16.06
Snow (D)	Humid (f)	0.37	0.57	3.61	5.75	10.46	0.02	20.78
	Dry Summer (s)	0.04	0.09	0.54	0.08	0.01	0.08	0.84
	Dry Winter (w)	0.33	0.00	1.92	0.29	0.53	0.55	3.61
	Subtotal	0.74	0.66	6.08	6.11	10.99	0.65	25.23
Polar (E)	Tundra (T)	0.00	0.00	0.00	0.03	0.01	0.00	0.04
	Frost(F)	0.16	0.27	1.77	1.42	1.10	0.71	5.43
	Subtotal	0.16	0.27	1.77	1.46	1.10	0.71	5.47
Total		4.40	3.21	22.95	33.06	32.64	3.73	100.00

discharge (Milliman and Syvitski, 1992; Syvitski and Milliman, 2007). The global lithological map (GLiM) is a product of 1,235,400 polygons representing 16 lithological descriptions that define the physical properties of Earth's land surface. This describes six main lithological categories according to Hartmann and Moosdorf (2012) as siliclastics (su, ss, py), carbonate-rich and evaporites (sc, sm, ev), volcanics (va, vi, vb), plutonics (pa, pi, pb), metamorphics (mt) and other (wb, ig, nd). Although second and third order classifications are available, these descriptive attributes of the rock lithology are not exhaustive on the global scale. The lithology of a catchment was similarly defined to that of the climate classification with a majority category classification given to each catchment region. Furthermore, a proportion of each lithology type within the catchment was given as percentage (0–100%).

3. Results

The GTSC database delineates 69,586 catchments to endorheic and exorheic sinks and 239,831 sub-catchments representing drainage patterns of the terrestrial sink for the global non-glaciated landmass (Figs. 2 and 3). Of these, 180,737 catchments (75%) are from source catchments with a surface area of 106×10^6 km^2 (82%) and 59,094 are then modern terrestrial sink catchments (25%) with a surface area of 24×10^6 km^2 (18%). Of the global non-glaciated land surface, source catchments drain 71×10^6 km^2 (67%) to a terrestrial sink.

Below we describe the geographical distribution and proportion of catchments as endorheic, exorheic, tectonic regime, climate, lithology, geometric attributes and sediment load.

3.1. Endorheic and exorheic distribution

The global endorheic catchment distribution represents 30×10^6 km^2 (23%) while the remaining 100×10^6 km^2 (77%) are exorheic catchments (Fig. 4). The proportion of endorheic basins differs significantly from previous works (e.g., Vörösmarty et al., 2000a at 13%) with the main differences being attributed to a larger endorheic extent of the Sahara Desert, southern Patagonia and Australia. Part of this is due to the higher resolution DEM model used by the HydroSHEDS delineation (Lehner et al., 2008), which is incorporated in our study and results in a similar endorheic basin distribution.

Of the 100×10^6 km^2 exorheic draining land surfaces, 35×10^6 km^2 are on epicontinental seaways (36%) with the remaining 65×10^6 km^2 (64%) draining to the continental shelf (Fig. 4). Geographically, the Atlantic Ocean represents the highest proportion of the total exorheic draining area (~20%), followed by the Indian Ocean (3.2%), the Pacific Ocean (3.2%) and the Arctic Ocean (<0.1%) (Appendix A).

The largest catchments draining to seas are the Kara Sea (7%), the Laptev Sea (3.5%), the Beaufort Sea (2.1%), the Arabian Sea (1.8%) and the East Siberian Sea (1.3%). Furthermore, the Gulf of Mexico (5%), the Gulf of Guinea (3.7%), the Gulf of St. Lawrence (1.6%), the Persian Gulf (1.2%) and the Gulf of California (1%) represent a large proportion of the world's exorheic draining landmass. With the exception of the Arctic Ocean, exorheic catchments draining to oceans generally tend to be associated with a large terrestrial sink component (Atlantic 12.5%, Indian 15%, Pacific 5.7% and Arctic < 0.1%). Epicontinental seaways and gulfs have more varied terrestrial sink contributions (Appendix A). The plate tectonic configuration at present is a main control on the endorheic, exorheic and epicontinental seaway distribution (e.g. Nyberg and Howell, 2016).

3.2. Tectonic distribution

Classifying catchments by their main terrestrial sink tectonic regimes shows a variable influence (Fig. 5). Aerially, 33% of catchments that drain to terrestrial sinks are intracratonic including significant portions of the African and Australian interior, northern Europe, the Caspian Sea, central Asia, southern South America and Northwestern Passages of Canada. Catchments associated with a foreland tectonic regime represent 28% with the majority contributed from the Asian continental landmass. Passive margins account for 27% of the catchment area and are concentrated around the shorelines of Africa, South American, the Atlantic Ocean, the Indian Ocean, and the Gulf of Mexico. Interior settings comprise 5.7% extensional settings including the Basin and Range, the United States, the central Andean region, the East African Rift and Lake Baikal extension, and Russia. Strike-slip catchments (4.2%) are present in central China and surrounding the Gulf of California region. Only 1.4% of the land surface drains to terrestrial forearc sinks that predominantly occur around the Pacific Rim margin (Fig. 5).

In contrast, the global exorheic catchments by shoreline tectonic regime (e.g., Nyberg and Howell, 2016) are dominated by passive continental margins draining 63% of the land surface to a majority of the coastlines of the Arctic, Atlantic, and Indian oceans. The contributing areas of intracratonic catchment settings drain 11.5%, including the Northwestern Passages and the Kara Sea of the Arctic Ocean, the Gulf of Carpentaria in Australia, the Persian Gulf from Saudi Arabia and sections of the Yellow Sea in China/Korea. Forearc settings, while contributing aerially a small portion of terrestrial sinks (Nyberg and Howell,
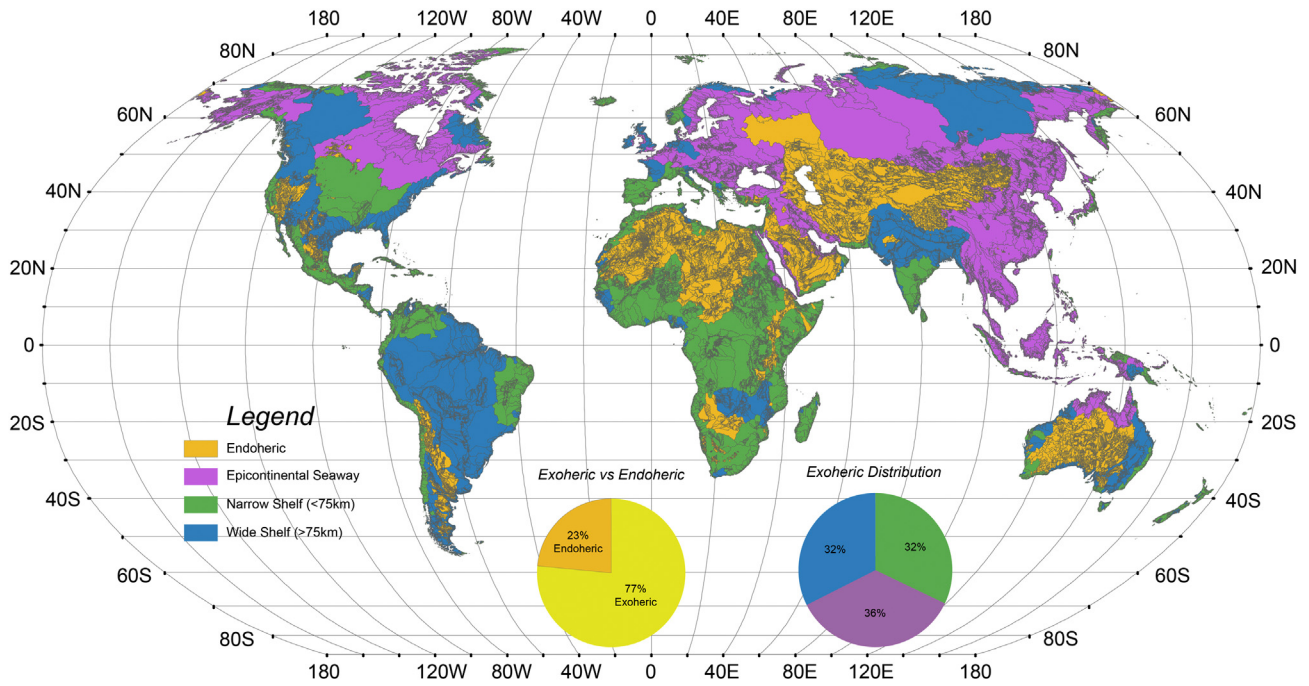
Fig. 4. Global exorheic and endorheic distribution of catchments. Distribution of catchments as exorheic and endorheic and further subdivided based on narrow shelf (<75 km), wide shelf (>75 km) and epicontinental seaways.

2015), contribute ~5% of the land surface area to the shoreline. Lastly, strike-slip and extensional regimes aerially comprise the least catchment surface area to ocean sinks at 2.8% and 2.2%, respectively.

The combined terrestrial, endorheic and exorheic catchment contribution by tectonic regime is summarized in Figs. 5 and 6. Intracratonic and passive margins play a most prominent role representing 33% each of the continental land surface. Foreland settings represent 23% followed by extensional and strike-slip settings at 4.4% and 3.7%, respectively. Forearc basins represent the least of the world's land surface area at a mere 3.2%. For the remainder of the article, analyses that refer to the tectonic classification utilize this terrestrial, endorheic and exorheic tectonic catchment classification.

Global passive and active continental shelf/slope margins represent 76% and 24%, respectively (Fig. 7). Extensional, forearc and strike-slip tectonic regimes are exclusively of active tectonic margins while intracratonic settings are exclusively passive. The drainage point of foreland tectonic catchments represents a significant proportion of passive settings at 53%, including parts of the Andean, Brook Range, Himalayan, Mackenzie, Zagros, Gulf of Thailand, Yellow Sea and interior Central Asia foreland basin systems. Active foreland margins contribute 47%,
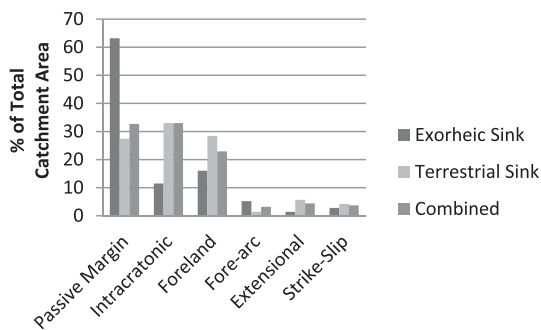
including significant parts of Indonesia and Malaysia, Central Asia, the Sea of Okhotsk, the Sea of Japan, the Mediterranean and portions of Alaska and the southern Andean mountain belts. Passive continental margins are primarily associated with passive oceanic margins (95%) with a small proportion draining along active ocean margins (5%) including the Red and Mediterranean seas.
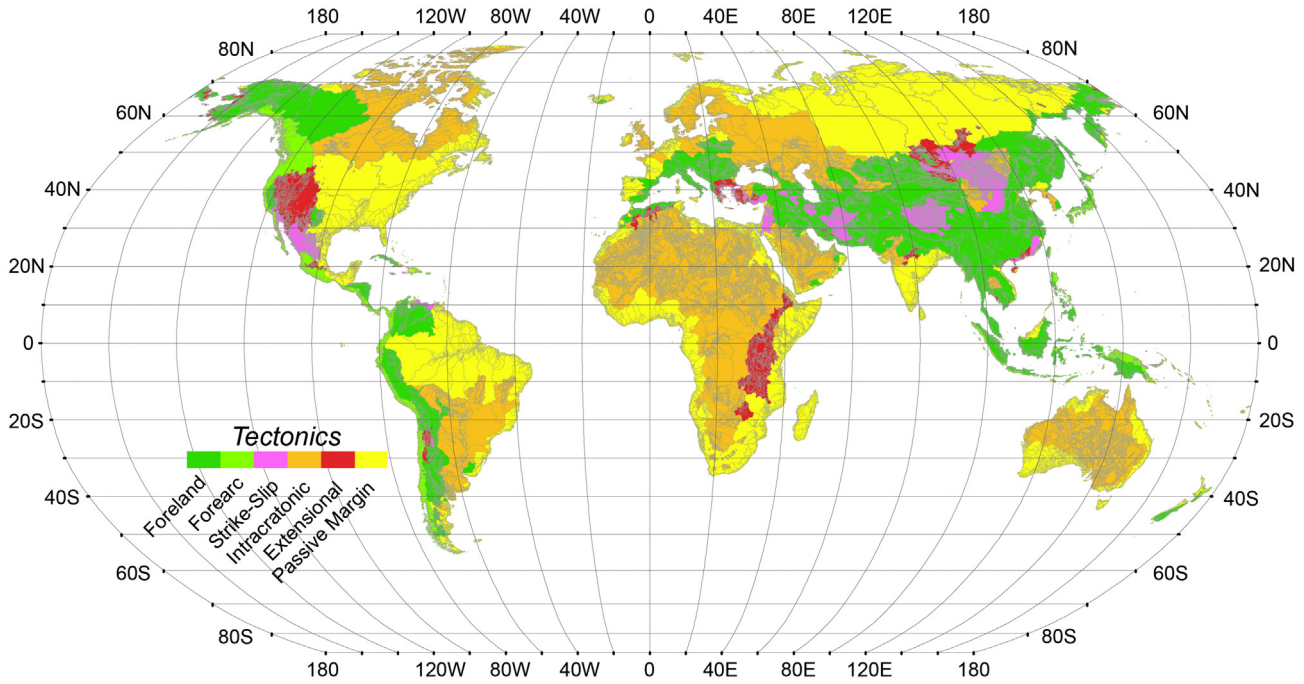
3.3. Climate distribution

Arid climates are the most aerially extensive (31%) and are found around the equatorial and mid-latitudes, including Australia, northern Africa, central Asia, the Middle East and western North America. Source catchments are however significantly less arid (24%) and are influenced by seasonal precipitation patterns of either dry summers (11%) or dry winters (13%; Appendix B). Snow or continental climate patterns represent the second highest proportion of catchments (25%) and drain mainly to the Arctic continental shelf, such as the Canadian Shield and the Siberian platform. Within the source catchment, snow climates are the most common representing nearly a third of the land surface (30%) with 25% of that region being fully humid (*f*), while only 1% and 4% are dry summers and dry winters, respectively (see Appendix B).

Equatorial climates of Central and South America, Australasia and the Pacific islands represent 22% of the non-glaciated landmass. The source catchments have an equatorial climate proportion of 23% with a majority associated with seasonal dry winters conditions (13%) followed by humid (5%), monsoons (4%) and dry summers (<1%). Warm temperate regions (16%) are distributed predominately along mid-latitude regions such as North America, Europe and southern South America. Within the source catchment, catchments are proportionally very humid (9%) although dry winters (4%) and dry summers (3%) are significant. Lastly, polar regions represent a small proportion of global climates (5% globally and <7% of the source catchment) and are mainly found in high altitude or high latitude regions such as the Himalayas, the Andes or the Arctic.

Table 1 summarizes the climatic distributions of catchments, which have been subdivided based on tectonics. The results show that extensional settings are dominated by either a dry winter (w) in equatorial

Fig. 5. Primary tectonic regime of global catchments by area. The proportion of catchments by area is defined by a tectonic model as terrestrial sinks, exorheic sinks and a combined tectonic model.
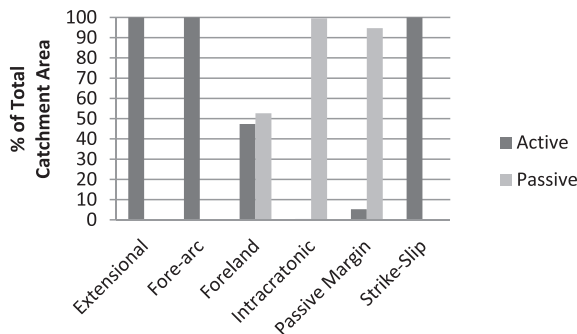
Fig. 6. The global distribution of catchments by tectonic regime. The classification of global river drainage catchments by its primary exorheic/endorheic and terrestrial sink tectonic classification. The tectonic classification of foreland, forearc, strike-slip, intracratonic, extensional and passive margin follow the schema used by Nyberg and Howell (2015) based on simplified nomenclature of Ingersoll (2012).

and warm temperate climates and by dry summers (s) in arid climates. Snow climates in extensional tectonic settings are evenly distributed between humid (f) or dry winters (w). Forearc catchments in equatorial and snow climates tend be humid, while those in arid or warm temperate settings are more evenly distributed between dry summers and dry winters (arid) and humid and dry summer (warm temperate) settings. In foreland settings, humid settings dominate catchments in equatorial, warm temperate and snow climates followed by a high dry winter climate contribution. In addition, monsoonal seasonality represents a significant proportion of equatorial regions.
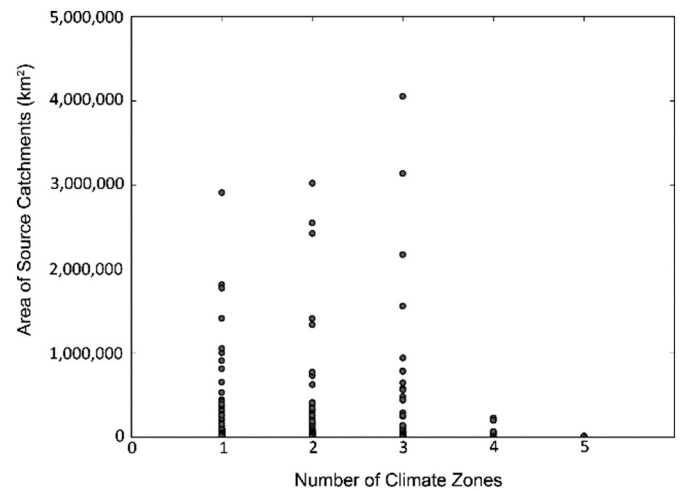
Intracratonic regimes of dry winter climates are predominately in equatorial and arid settings, whereas warm temperate and snow environments are largely humid. Passive margins are similarly dominated by dry winters in equatorial and arid climates, while warm temperate and snow climates are mainly humid. Furthermore, equatorial climates of passive margins are documented with monsoonal conditions. Strike-slip tectonic regimes are the least significant, and are mostly found in arid and snow climate conditions with dry summers and dry winters. No discernable trends in the number of climates that influence a catchment and its size can be detected in the current database (Fig. 8).

3.4. Lithology

The global distribution of source catchment lithology by tectonic regime shows a variable contribution to terrestrial sinks (Fig. 9). Extensional and strike-slip tectonic source catchments are the most diverse lithologically. Extensional settings are composed of the largest volcanic (va, vb, vi) contribution (17%) of all tectonic regimes, whereas siliclastic material (su, ss, py) are the least (35%). High carbonate rich/evaporites (sc, sm, ev) content (18%) followed by plutonics (pa, pi, pb; 8%) and metamorphics (mt; 12.5%) and other (wb, ig, nd; <1%). Strike-slip catchments are at present dominated by lithologies of carbonate rich sources (>50%) while the remaining are siliclastics (28%), volcanics (10%), plutonics (5%), metamorphics (3.2%) and other (<3%).

Fig. 7. Proportion of global catchments by area within each tectonic regime that have an active or passive continental shelf/slope margin.

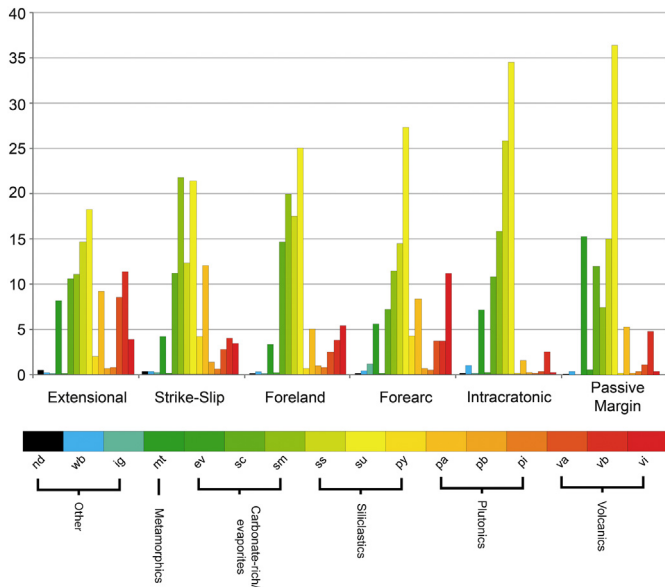**Fig. 8.** Number of climate zones by source catchment area. The number of climate zones as defined by the Köppen-Geiger classification and contributing source catchment size to a terrestrial sink where the climate represent at least 15% of the total catchment area.

Fig. 9. Lithological composition of source catchments by tectonic regime. Average lithology distribution of source catchments in percentage by tectonic regime based on the GLiM database of Hartmann and Moosdorf (2012). nd - no data, wb - water body, ig - ice and glaciers, mt - metamorphics, ev - evaporites, sc - carbonate sedimentary rocks, sm – mixed sedimentary rocks, ss – siliclastic sedimentary rocks, su – unconsolidated sediments, py – pyroclastics, pa – acid plutonic rocks, pb – basic plutonic rocks, pi – intermediate plutonic rocks, va – acid volcanic rocks, vb – basic volcanic rocks and vi – intermediate volcanic rocks.

Intracratonic and passive margin source catchments have a higher siliclastic and metamorphic content. Passive margins are represented by siliclastics (63%), metamorphics (15%), carbonates (12%), plutonics (3%) and volcanics (<2%). Intracratonics are represented by siliclastics (52%), carbonates (25%), metamorphics (17%), plutonics (3%) and volcanics (<2%). Foreland settings have a similar high siliclastic content (50%) with a high carbonate content (33%) and a higher volcanic proportion (5%) while metamorphics (4%) and plutonics (4%) are both low. Finally, forearc settings show a high siliclastic (65%), carbonate-rich (13%), plutonics (7%), volcanic content (5%) and a low metamorphic distribution (1%).

Spatially, the lithology of terrestrial sinks source catchments differ as well (Fig. 10). Passive margins along the Americas, Australia and Europe contain a high proportion of unconsolidated sediments and siliclastic sedimentary rocks whereas passive margins on the African continent contains a higher proportion of metamorphics and a higher volcanic content on the Indian plate. Foreland settings along the Sunda shelf, Himalayas and Sea of Okhotsk have a high volcanic influence with less unconsolidated siliclastic content. Strike-slip (e.g., Gulf of California) and extensional tectonic regimes (e.g. Basin and Range, East African rift system) have the highest volcanic content. Finally, intracratonic settings of the interior Australian and African continents demonstrate a high unconsolidated sediment and siliclastic sedimentary rock content similar to that of passive margins though a lower proportion of metamorphics and volcanics.

3.5. Geometrical characteristics

We describe below the geometrical characteristics of source catchment area, width and relief by tectonic regime for the GTSC dataset.

3.5.1. Catchment area

The number of source catchments decreases logarithmically with catchment area, though the nature of the relationship differs between tectonic regimes (Fig. 11). Passive margins show the lowest power law constant and exponent suggesting a greater proportion of large
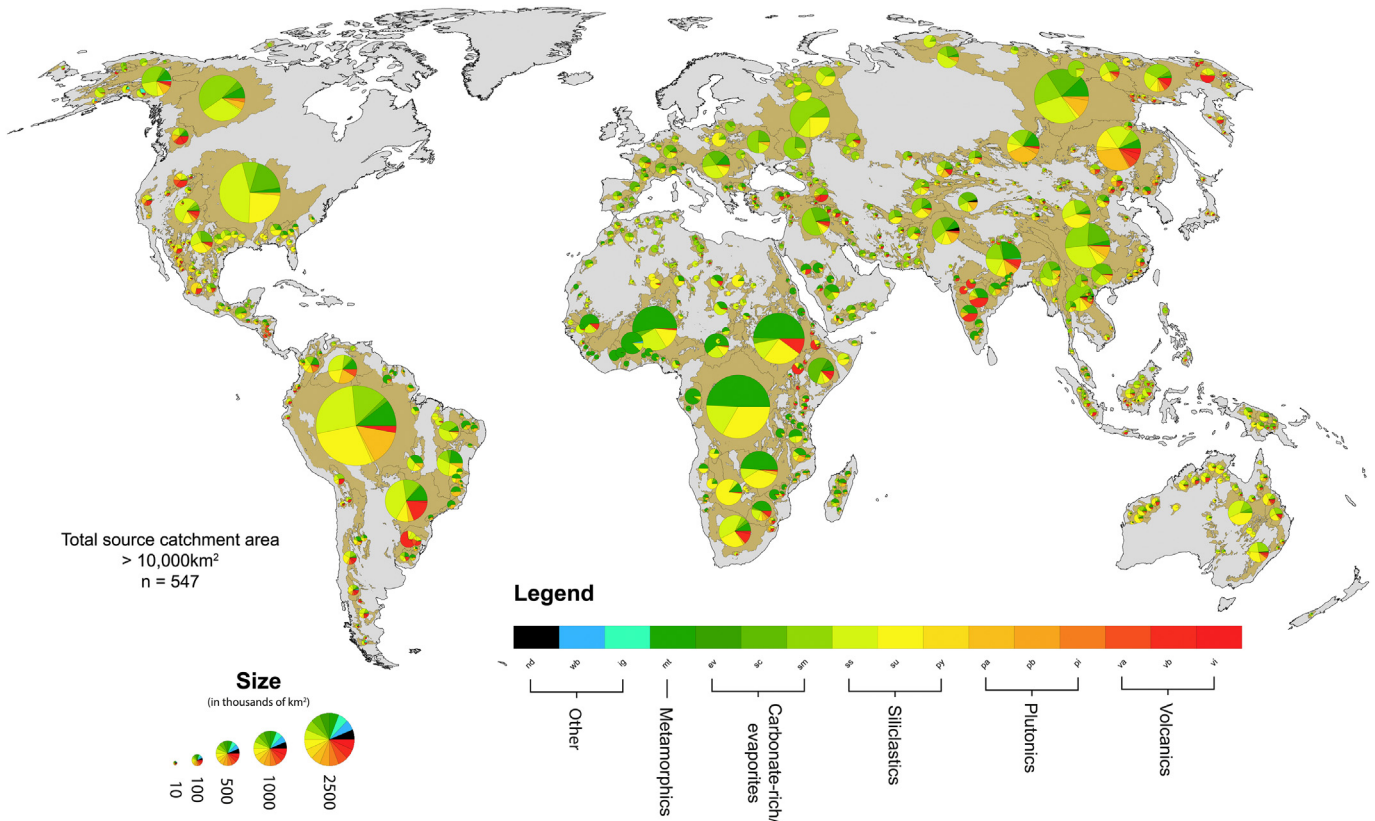
Fig. 10. Geographical distribution of source catchment lithology. Lithology of source catchments draining to a terrestrial sink for the largest drainage source catchments (>10,000 km²). The size of the pie chart reflects the size of the source catchment drainage area. Lithology classification after the GLiM by Hartmann and Moosdorf, (2012, see Fig. 9).
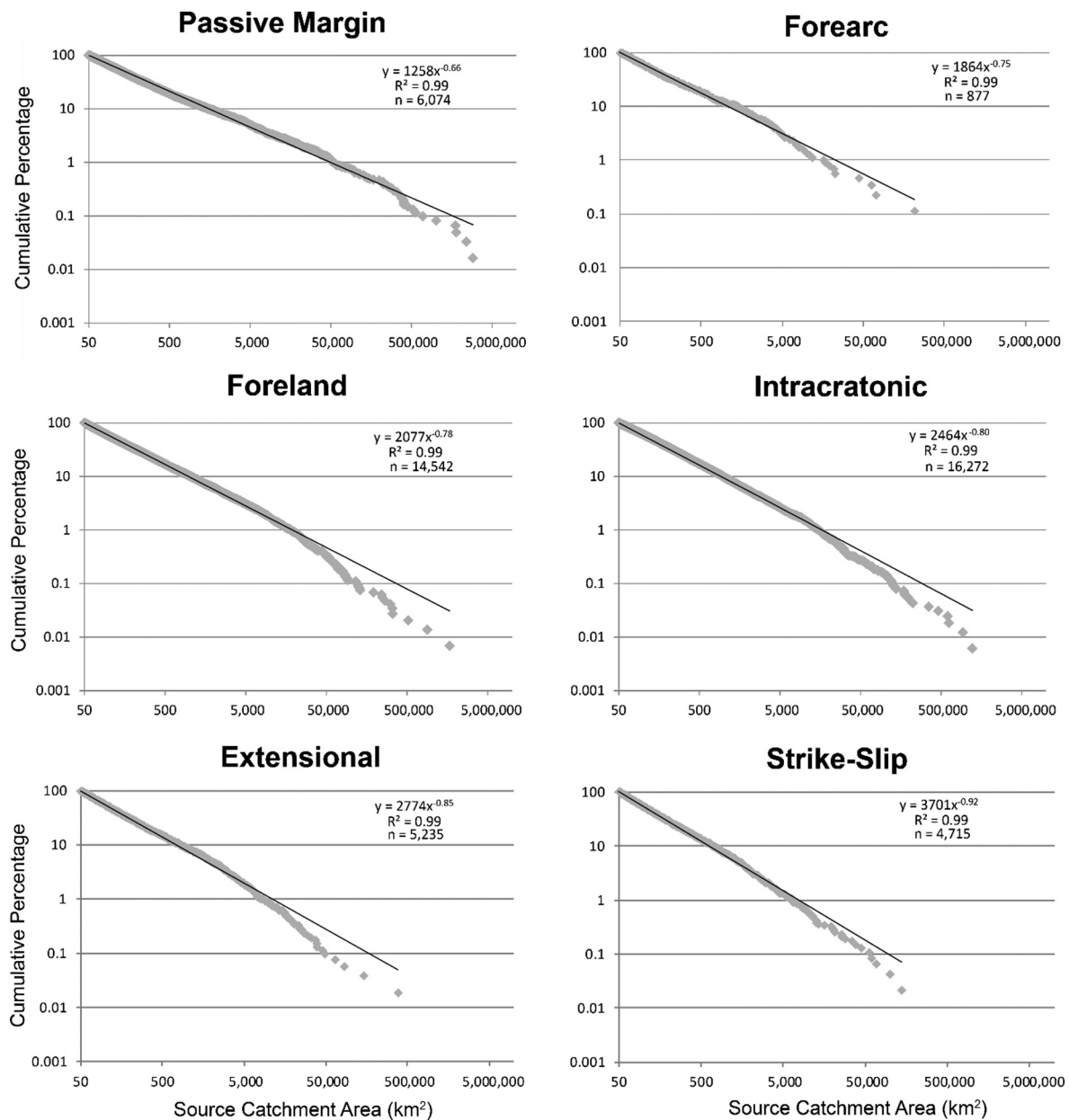
Fig. 11. Cumulative percentage of source catchments by catchment size. Data shows a power-law relationship between the number and size of catchments across the range of tectonic regimes for source catchments > 50 km². Note the varying power-law function amongst the different tectonic regimes.

source catchments. In comparison, intracratonic, extensional and strike-slip settings have a low proportion of large source catchments.

Plotting the cumulative percentage of source catchments by source catchment size for each individual exoheric/enorheic drainage show comparable power-law relationships by tectonic regime (Fig. 12). This shows that given the size of a source catchment, the number and size of source sub-catchments to a particular terrestrial sink can be estimated.

The size of a catchment is related to its river length draining to its lowest endorheic or exorheic point (i.e., Fig. 1A) by a power law relationship (Fig. 13A) following Hack's law (Hack, 1957). A similar relationship exists between source catchment river length and source catchment area draining to terrestrial sinks (Fig. 13B), reiterating the validity of defining source catchment area from river length (and vice versa, Rigon et al., 1996).

The size of the largest source catchment as a percentage of the entire catchment area is shown in Fig. 14. The results show that extensional,

foreland, intracratonic and strike-slip tectonic regimes have positive skewness of 0.63, 0.42, 1.18 and 0.68 and a mean size of 36%, 40%, 27% and 33%, respectively. Forearc and passive margins have a negative skewness at −0.37 and −0.56 and a mean size of 62% and 65% of the total catchment area, respectively.

The number of source catchments that represents at least 1% of the total source catchment area is shown in the box plots in Fig. 15. The results show a large variability within, and significant overlap between tectonic regimes. The fewest source catchments draining to terrestrial sinks occur in passive margins and forearc settings, with a mean of 6.3 (±4.4) and a median of 5 for the passive margins, and a mean of 6.7 (±4.8) and a median of 5 in the forearc settings. Foreland and intracratonic regimes show means of 9.0 (±6.1) and 9.6 (±6.1) and a median of 7 and 8, respectively. Finally, extensional and strike-slip settings have the largest number of source catchments draining to terrestrial sinks, with means of 11.6 (±7.0) and 12.5 (±7.3) and a median of 10 and 11, respectively.
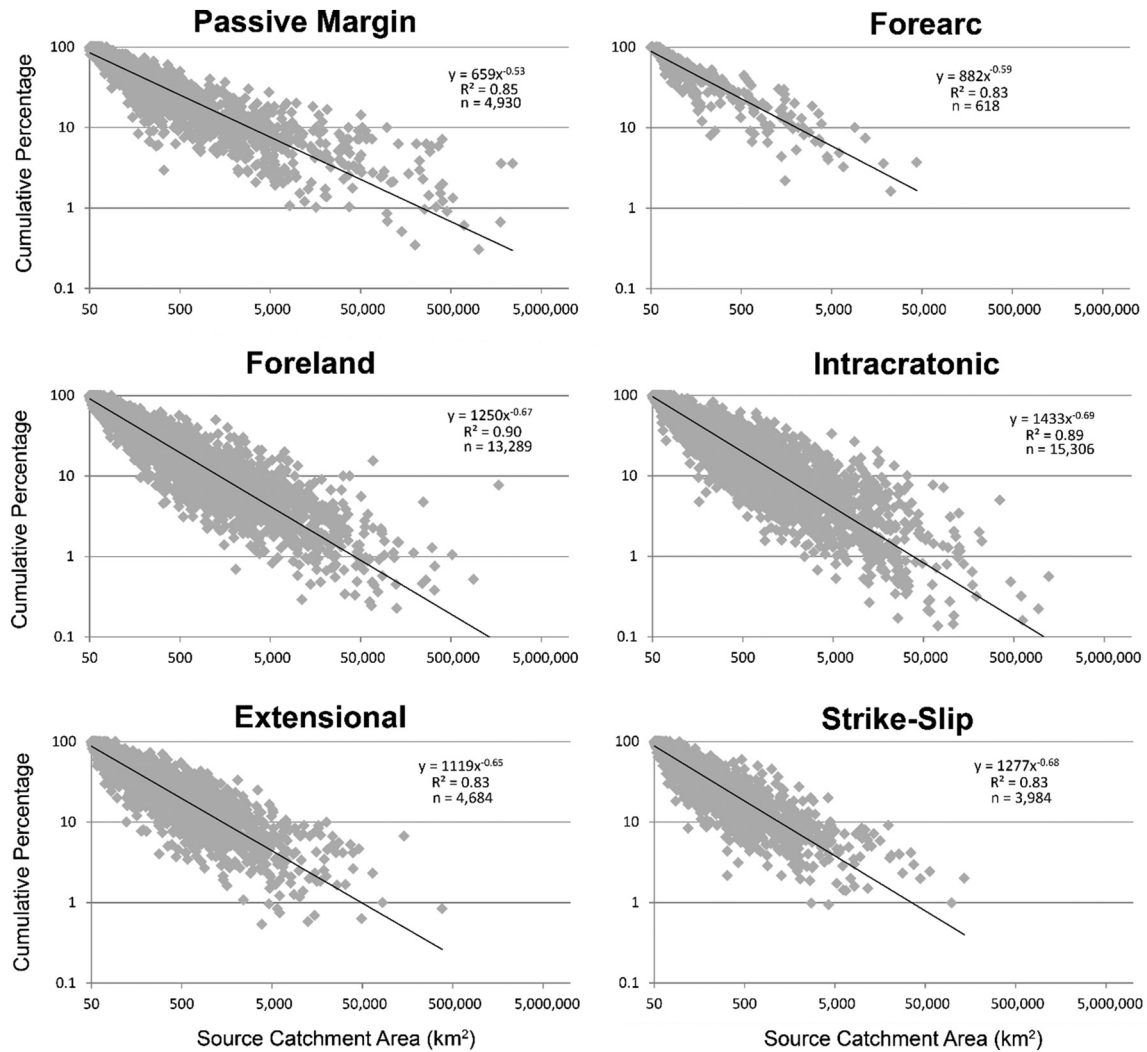
Fig. 12. Cumulative percentage of source catchments by catchment size for individual terrestrial sink systems. Data shows power-law relationship between the number and size of catchments across the range of tectonic regimes for source catchments > 50 km² that drain to a terrestrial sink. Note the varying power-law function amongst the different tectonic regimes.

Of those source catchments that drain to a terrestrial sink, the size of the terrestrial sink in relation to its total catchment area is summarized in Fig. 16. The results show that passive margins have the smallest relative terrestrial sink with an average of 14% (±20.8) of its total catchment area. Forearc settings are represented at 15.6% (±24.7), extensional settings at 26.1% (±24.7%), foreland settings at 27.1% (±25.1), strike-slip at 38.2% (±21.7) and intracratonic at 44.3% ±30.1).

3.5.2. Catchment width

Source catchment width shows a power-law relationship with the length of its longest river (Fig. 17). The results suggest that smaller source catchments, that are typical along active tectonic margins (e.g. Fig. 11), have on average a higher width to length ratio. Intracratonic settings which are similarly characterized by smaller source catchments (e.g. Figs. 11 and 14) and are characterized by a higher width to length ratio. In comparison, passive margins and foreland settings have a lower width to length ratio that reflect the absolute size of their largest source catchments.

3.5.3. Relief

The variability of relief amongst the different tectonic regimes for the distribution of global catchments is summarized by the box plots in Fig. 18A. Forearc tectonic regimes are characterized by the highest elevation of 1.9 km (±1.3), with foreland at 1.4 km (±1.3), extensional at

1.1 km (±0.75, strike-slip at 0.99 km (±0.72), passive margins at 0.64 km (±0.84) and intracratonic at 0.3 km (±0.52). The range of elevation within the sinks by tectonic setting is defined in Fig. 18B. The results show that extensional and strike-slip settings have the highest elevation range with a mean of 742 m (±530) and 505 m (±467) followed by foreland basins with a mean of 346 (±471). Forearc, intracratonic and passive margins are characterized by low relief with a mean of 198 (±195), 171 (±168) and 162 (±195), respectively. On average, the elevation change between the sink and source catchment is 17.9 times for forearc settings, 8.9 for foreland settings, 7.3 for passive margins settings, 2.8 for strike-slip settings, 2.6 for intracratonic settings and 2.4 for extensional settings.

3.6. Sediment load

The influence of lithology, area, relief and temperature on the calculation of sediment load based on BQART (Eq. (1); Syvitski and Milliman, 2007) show that source catchments account for a majority of sediment transport across the spectrum of tectonic regimes (Fig. 19). However, an examination of the maximum total suspended sediment load contribution from a single source catchment within the larger exorheic/endorheic catchment (e.g., Fig. 1B) shows variance by tectonic regime (Fig. 20).

A

B
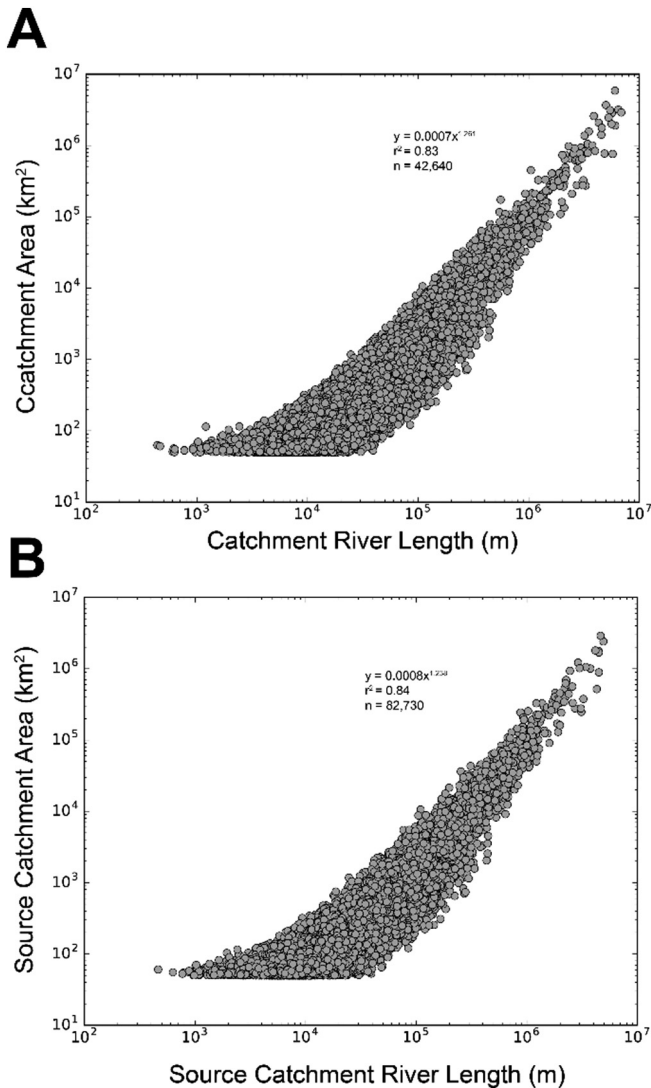
Fig. 13. Relationship between catchment river length and catchment area. (A) shows the power-law relationship between river length and area for catchments draining to an exorheic or endorheic point. (B) shows the power-law relationship between river length and area for source catchments draining to a terrestrial sink. Catchments are shown with an area > 250 km².

On average, forearc (64%) and passive (63%) margins have one source catchment contributing about two-thirds of the total suspended sediment load (Fig. 20). Foreland settings have a single source catchment contribution to the terrestrial sink of approximately 50%, while intracratonic settings contribute 43%. The average maximum contribution from a single source catchment is the least for extensional and strike-slip source areas (both are 36%). In addition, foreland, intracratonic, extensional and strike-slip tectonic regimes show a varied range of maximum contributing sediment load from the main source catchment. This suggests that numerous source catchments have a potential contribution to the total sediment load of rivers to the oceans in those tectonic regimes. This, in turn, will influence along-strike variability of source catchment sediment discharge and sediment composition in the terrestrial sink (Weltje, 2012).

3.6.1. Sediment load versus climate/tectonics

Table 2 maps the total suspended sediment load by climate. Proportionally within equatorial climates, extensional, forearc, foreland and passive margins have a high representation of their total global contribution. Extensional and passive margins are mainly characterized by dry equatorial winter climates. The highest sediment contribution in

forearc and foreland settings is in humid equatorial climates, while passive margins also have a significant contribution. Monsoonal climates are important in foreland and passive margin tectonic regions.

Of the arid climates, all tectonic settings make a significant contribution. Dry winters are most prevalent of all tectonic regimes (e.g., intracratonic regimes 9.66% vs 2.21%) with the exception of extensional settings where dry summers dominate (0.94% vs 0.51%). Dry winters in forearc and strike-slip tectonic regimes are twice as prevalent as dry summers. Foreland and passive margin settings have a relatively even contribution from both dry winters and dry summers.

In warm temperate settings, foreland and passive margins contribute a significant proportion to the total suspended sediment load. Foreland settings tend to be characterized by dry winters (6.96%), whereas passive margins are in humid regions (3.55%). Extensional and forearc settings are evenly distributed in humid, dry summer and dry winter conditions. Snow climates are mainly characterized by either foreland (2.62%) or passive margin (1.29%) regimes with humid conditions. Finally, polar climates are primarily characterized by frost conditions in foreland settings (2.26%) of high altitude regions such as the Himalayas.

4. Discussion

The global distribution of the coupled source catchments and their terrestrial sinks have implications for a wide range of topics such as water-atmospheric interactions, biogeochemical cycles, socio-economic concerns, geomorphological processes and understanding the controls on the stratigraphic record. In this discussion, we will focus our attention on the implication of the results from a geomorphological and sedimentological viewpoint. First, we describe source catchment characteristics by morphology, outlet spacing, lithology and climate for different tectonic regimes. Second, we describe the influence of source catchment characteristics on sediment discharge to the terrestrial sink. Finally, we discuss the implications of the source catchment influence on the terrestrial sink for sediment signal propagation to the marine realm on geological timescales (>10^4 yr) that characterize source-to-sink systems.

4.1. Source catchment morphology

Catchments with strike-slip tectonic regimes are characterized by a relatively larger terrestrial sink in comparison to the total catchment area with numerous wide but small source catchments (Figs. 12, 14–17). Relief of the source area for strike-slip regimes is on average up to 2.8 times higher than the terrestrial sink (Fig. 18). Extensional settings show a similar set of characteristics but a more varied terrestrial sink area in comparison to the total catchment area, reflecting a range in basin maturity (Figs. 14, 16, 20). Extensional settings show a median of 11 source catchments (Fig. 15), second only to strike-slip tectonics, and a source catchment relief 2.4 times higher than the terrestrial sink (Fig. 18). The lower source catchment:terrestrial sink relief ratio of strike-slip and extensional settings (2.8 and 2.4 times, respectively) reflect the higher relief alluvial fans that comprise the terrestrial sink. The largest contribution of total suspended sediment load from a single source catchment is relatively low for both tectonic regimes (Fig. 20).

On average, foreland regimes are characterized by slightly fewer (i.e., median = 7) and narrower source catchments that feed a larger terrestrial sink with relief 8.9 times greater than the terrestrial sink (Figs. 12, 14–18). The large absolute size of foreland source catchments explains the source catchment elongation (Fig. 17) as catchments narrow with increasing size due to the limited amount of available space (Hack, 1957; Rigon et al., 1996). The suspended sediment load derived from a single source catchment is more varied than extensional and strike-slip tectonic regimes but remains small (Fig. 20), suggesting that the total suspended sediment load of the total catchment area is the contribution from its numerous source catchments. Intracratonic settings are representative of the largest relative terrestrial sink area
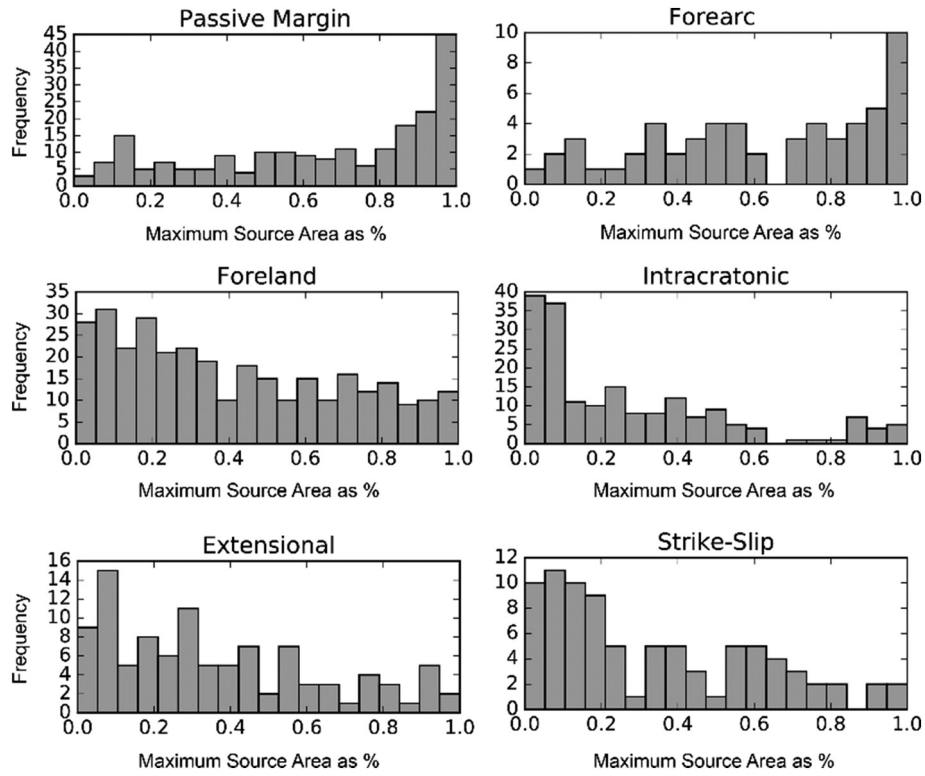
Fig. 14. Histogram distributions of the largest contributing source catchments draining to terrestrial sinks (as a percentage of the entire source catchment region) in different tectonic settings. Based on source catchments with a total suspended sediment load > 1 MT/yr.

but are otherwise similar in characteristics to strike-slip and extensional settings, with numerous wide and small source catchments (Figs. 12, 14–17). Source catchment:terrestrial sink relief ratio is also similar to strike-slip and extensional settings at 2.6, although the absolute source catchment relief is significantly lower (~<500 m; Fig. 18A).

Passive margins and forearc tectonic regimes generally have the smallest terrestrial sink area relative to the total catchment area

Fig. 15. Box plots showing the number of source catchments contributing to terrestrial sinks by tectonic regime. The boxes indicate the 25th and 75th percentiles, the whiskers show the 10th and 90th percentiles, the square shows the mean, and line shows the median.

(Fig. 16). The terrestrial sink is fed by a few relatively large and narrow catchments and the change in relief between the terrestrial sink and source catchment is significant, on average 17.9 times for forearc settings and 7.3 times for passive margins (Figs. 12, 14–18). The largest source catchment in forearc settings and passive margins contributes a majority of the sediment production to their terrestrial sinks (Fig. 20). However, as peak discharge following a storm event increases with increasing catchment width (e.g., Sólyom and Tucker, 2004), the narrower morphology of passive margin and forearc source catchments will decrease the peak discharge at their terrestrial sinks in comparison to foreland, intracratonic, extensional or strike-slip settings.

The spacing of source catchments depends on source catchment area given that there is a limited amount of area for catchments to occupy along a mountain belt. Considering that source catchment area is related to river length (Fig. 13B) following Hack's Law (Hack, 1957), the width of the mountain belt, and thus the maximum river length, controls catchment spacing (Hovius, 1996; Sømme et al., 2013). Hovius (1996) observed that the spacing of catchments along linear mountain belts of active orogens is approximately half of the width of the mountain belt. In this study, the power-law relationship between the cumulative number of source catchments and source catchment size (Fig. 12) further suggests an internal distribution in source catchment sizes and thus an internal distribution in source catchment spacing. In other words, there exists a spacing of source catchments at the mountain belt scale and at smaller internal scales between the larger source catchments. This would be expected considering that smaller source catchments are similarly constrained by the available space between the larger source catchments.

Interesting, the power-law relationships showing the number of source catchments and size in Fig. 12 differ between active margins of strike-slip, extensional and foreland settings versus passive margins and forearc settings. This implies that passive margins and forearc settings are represented by a proportionally greater number of larger source catchments, and hence a larger spacing between those source
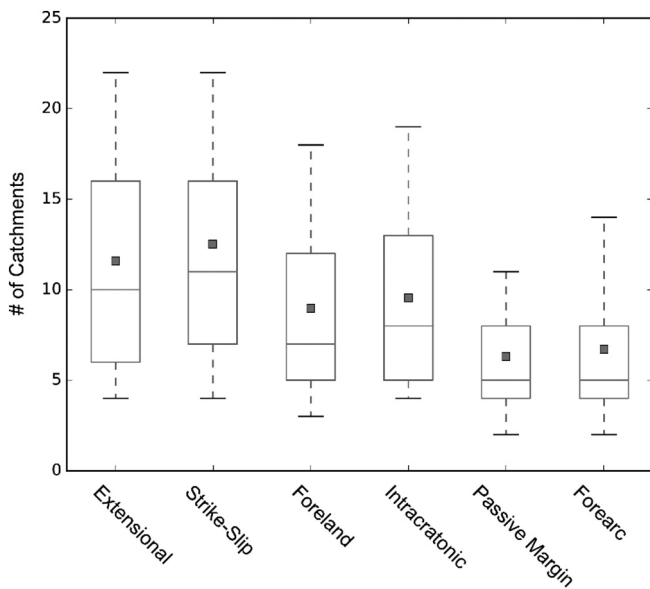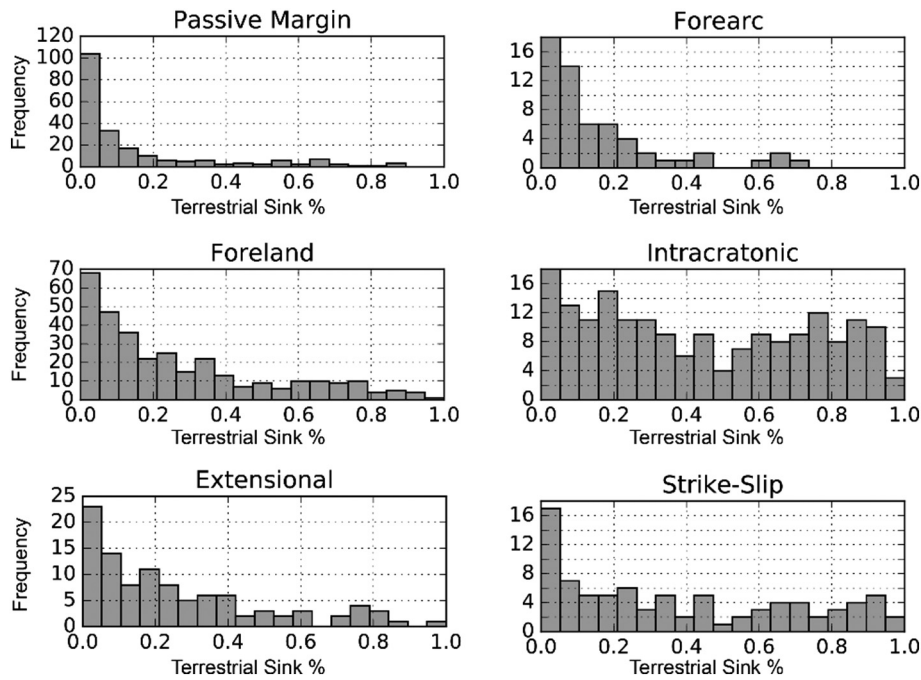
Fig. 16. The proportion of the exorheic/endorheic catchment as a terrestrial sink by tectonic regime. The proportion of the exorheic/endorheic catchment region that is represented as a terrestrial sink for global catchments with a total suspended sediment load > 1 MT/yr.

catchments in comparison to strike-slip, extensional and foreland settings. This will result in a lower spacing ratio (half width of mountain belt/source catchment spacing) than the narrow range of 1.91 to 2.23 as observed by Hovius (1996). It is important to note that Hovius (1996) only mapped source catchments along active linear mountain belts, whereas the current study considers source catchments across all tectonic regimes. In addition, the current study relates source catchments to the terrestrial sink, which may not necessarily be situated at the base of a mountain belt (i.e., passive margins). Source catchment spacing in relation to the terrestrial sink, however, is important because it controls the apices of fluvial systems that have preservation potential (Hovius, 1996; Nyberg and Howell, 2015). The spacing of those source catchments will influence the architecture of the preserved stratigraphic record as Owen et al. (2017) noted for a Palaeocene/Eocene distributary fluvial succession in an intermontane foreland basin of the Bighorn basin, Wyoming, USA.
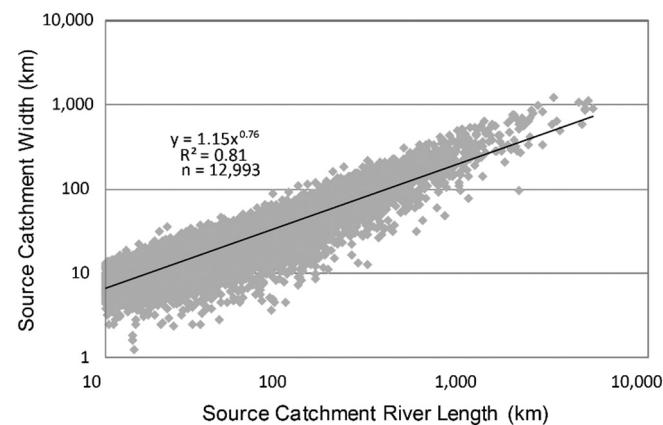
Fig. 17. Power-law relationships between source catchment river length and width. The power-law relationship show source catchments typically narrow with increasing catchment length. Catchments are shown with a river length > 10 km.

4.2. Source catchment lithology

The lithology of a source catchment will control denudation rates and sediment discharge to the terrestrial sink (e.g., Arribas and Tortosa, 2003; Palumbo et al., 2009; Norton et al., 2011). Lithologies that describe modern extensional and strike-slip source catchments associated with active young basin lifespans (Ingersoll, 2012) are varied and contain a high proportion of siliclastics, carbonates, volcanics and plutonics (Fig. 9). Source catchments of foreland and intracratonic tectonic regimes, in contrast, have a more uniform lithology distribution of siliclastics and carbonates (Fig. 9), which may reflect their longer lived sedimentary basins (Ingersoll, 2012). A more varied provenance distributed through numerous smaller source catchments will introduce along-strike variability in sediment discharge and composition to the terrestrial sink (Fig. 21).

The majority of forearc settings and passive margins are characterized by a few large source catchments (Figs. 15, 20), suggesting a lower along strike variability of sediment discharge and composition from different source catchment outlets to the terrestrial sink (e.g., Weltje, 2012; Fig. 21). Forearc settings show a higher percentage of volcanics, whereas passive margins have a higher proportion of metamorphics at present. A majority of large passive margins source catchments are furthermore characterized by high percentages of siliclastic lithologies (Figs. 9 and 10) that may indicate a large transport zone from hinterland to terrestrial sink (e.g., Fig. 22B).

The influence of source catchment morphology and lithology on sediment discharge along-strike of the terrestrial sink is illustrated in Fig. 21 for different tectonic regimes. Given three catchments (1, 2 and 3) in an extensional setting (Fig. 21A), foreland setting (Fig. 21B) and passive margin setting (Fig. 21C), each respective catchment has a similar proportion of siliclastics, metamorphics and volcanics regardless of tectonic regime as illustrated by the ternary diagram (Fig. 21). However, the different source catchment morphologies that define each tectonic regime (see Section 4.1) will influence the dominant control on the terrestrial sink. Extensional or foreland settings (Fig. 21A and B) composed of numerous equally contributing source catchments have a high
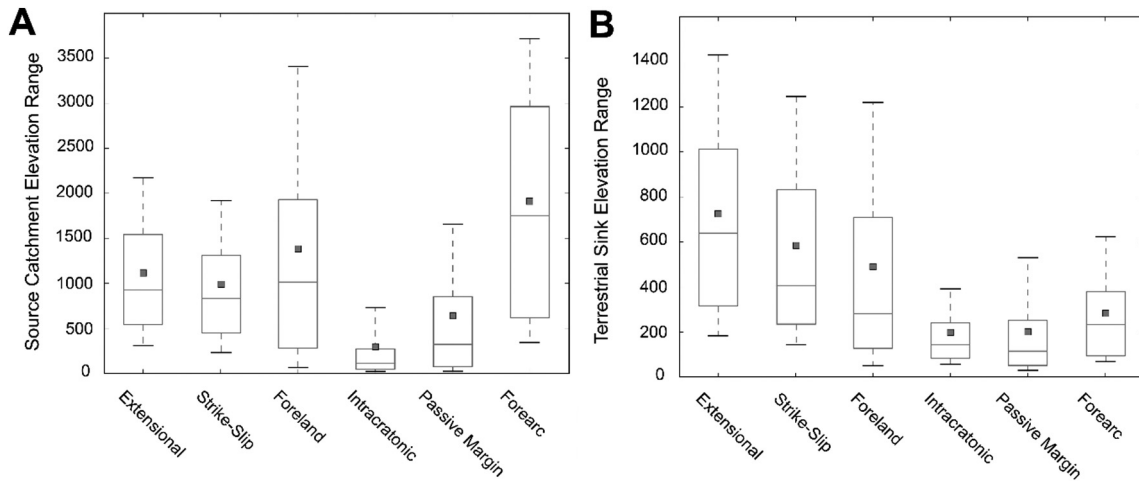
Fig. 18. Box plots showing the distribution of maximum catchment relief by tectonic regime. (A) shows the relief of the entire endorheic/exorheic catchment (Fig. 1A), while (B) shows the relief of the terrestrial sink by tectonic regime (Fig. 1B). The boxes indicate the 25th and 75th percentiles, the whiskers show the 10th and 90th percentiles, the square shows the mean, and the line shows the median.

potential for along-strike variability in terrestrial sink composition and sediment discharge in comparison to a single dominant source catchments that influences the entire passive margin terrestrial sink (Fig. 21C).

4.3. Source catchment climate

Seasonal dry winters or summers in the contributing source catchments influencing a majority of extensional and strike-slip tectonic regimes (Table 1) will cause infrequent higher magnitude discharge events. Meybeck et al. (2003) showed the higher temporal variability of global daily sediment discharge from smaller versus larger catchments. The high proportion of arid climates in tectonically active small catchments (Table 1) is a result of the present-day geographical distribution of continental plates (Nyberg and Howell, 2015) and the

orographic shielding influence of intermontane basins from steady precipitation (Roe, 2005; D'Arcy and Whittaker, 2014).

In contrast, terrestrial sinks of forearc and foreland tectonic regimes, situated at the base of mountainous ranges of converging plate tectonics, have a higher proportion of humid climates, though seasonal monsoonal and dry winters and dry summers are also important (Table 1). The windward flank of the orogenic range typically receives higher precipitation than its leeward side and variability of seasonal trade-winds (Roe, 2005) result in variable precipitation (Wulf et al., 2010). The small source catchments of the high relief, equatorial forearc tectonic regimes, yield high sediment load to the oceans (Milliman and Syvitski, 1992), with a short temporal lag response between precipitation and discharge (Meybeck et al., 2003). The short temporal response to precipitation in foreland settings associated with larger terrestrial sediment basins (Fig. 16) produces rapid sediment deposition as
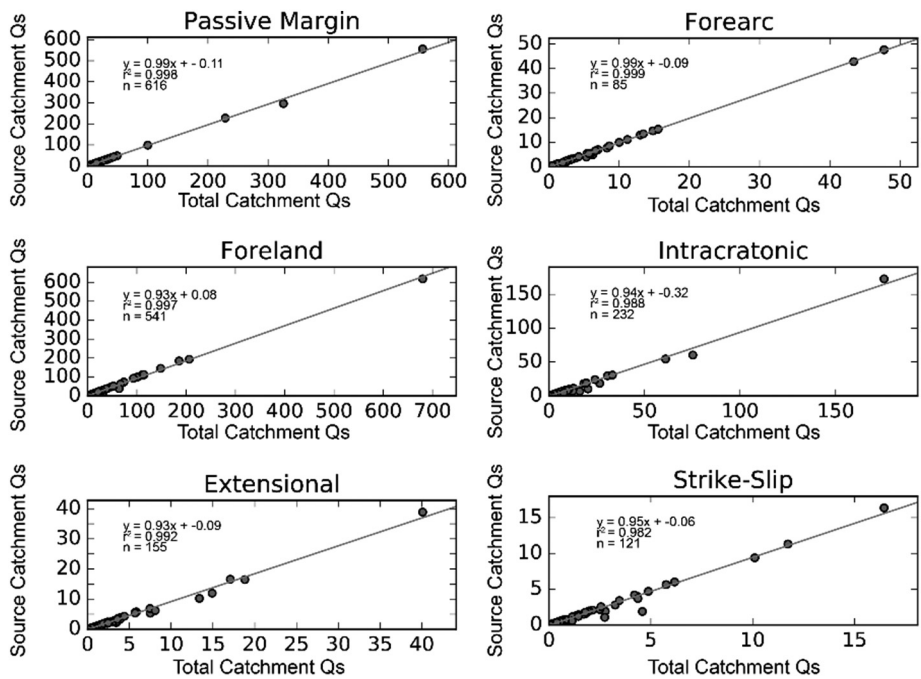
Fig. 19. Relationship of sediment load from contributing source catchments and the total catchment area. Total suspended sediment load (Qs) calculated based on BQART for the total catchment area (Fig. 1A) and contributing source catchments (Fig. 1B).
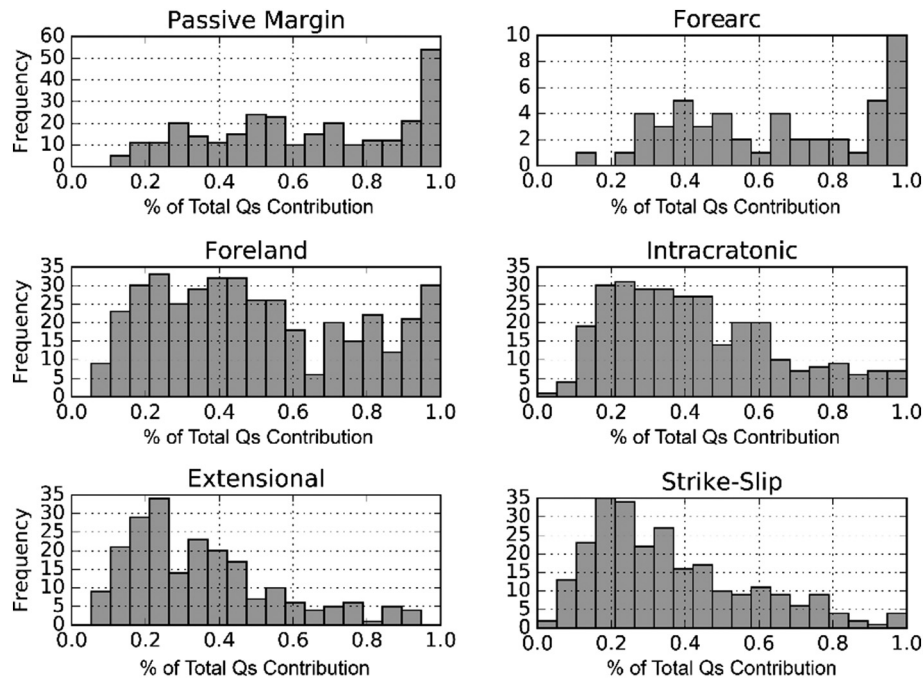
Fig. 20. Histograms showing the total suspended sediment load (Qs) contribution from the largest source catchment. The largest contribution from source catchment to each terrestrial sink is expressed as a percentage of the entire source catchment Qs load for endorheic/exorheic catchments with a Qs > 1 MT/yr.

terrestrial fans. Such fans have been well documented in literature (DeCelles and Cavazza, 1999; Leier et al., 2005; Weissmann et al., 2015).

Source catchments of passive margins have a more varied climatic contribution (Tables 1 and 2) as their terrestrial sinks are typically not associated on the flank of a mountain belt and the present-day distribution of passive margins that span a wide range of latitudes (Fig. 2). The terrestrial sink climate may thus be significantly different than its source catchment that spans a large distance and are associated with climatic influence from orogens. In fact, arid climates represent 60% of the surface area of present-day terrestrial sinks (Nyberg and Howell, 2015), nearly twice that compared to the surface area of arid climates in global catchments at 31% (Table 1).

No relationship is observed between the number of climate zones and the size of a source catchment (Fig. 8). This shows that the partial

independence between catchment area and water discharge (Syvtiski and Milliman, 2007) is not explained solely by larger catchments incorporating a larger variety of climates. Regional topography appears to be an important factor controlling the distribution of source catchment climates (Roe, 2005). Topographic influence may introduce a similar along-strike variability in sediment discharge to the terrestrial sink as source catchment lithology. The lithologies represented in Fig. 21 may be substituted for climates of arid, equatorial and warm temperate and each climate may be assumed to produce a different sediment discharge. Thus, systems characterized by numerous smaller source catchments (e.g., extensional, strike-slip, foreland and intracratonic settings) would show a high along-strike variability in sediment discharge at the terrestrial sink (Fig. 21A and B). In comparison, the terrestrial sink of systems characterized by fewer larger source catchments (e.g., forearc

Table 2
The relative contribution to the global total suspended sediment load in percentage by climate and tectonic regime subdivision for the GTSC database.

Climate		Tectonics						
First-order climate	Second-order climate	Extensional	Fore-arc	Foreland	Intra-cratonic	Passive margin	Strike-slip	Subtotal
Equatorial (A)	Humid (f)	0.01	3.10	5.70	0.15	3.46	0.14	12.55
	Monsoon (m)	0.04	0.54	2.16	0.21	2.03	0.02	4.99
	Dry Summer (s)	0.08	0.11	0.03	0.19	0.53	0.03	0.97
	Dry Winter (w)	1.10	1.16	2.44	2.43	5.97	0.45	13.54
	Subtotal	1.23	4.90	10.32	2.97	11.99	0.64	32.05
Arid (B)	Dry Summer (s)	0.94	0.62	3.48	2.21	4.11	0.85	12.21
	Dry Winter (w)	0.51	1.75	4.67	9.66	5.52	1.74	23.85
	Subtotal	1.45	2.37	8.15	11.87	9.63	2.59	36.06
Warm Temperate (C)	Humid (f)	0.43	0.61	3.33	0.74	3.55	0.08	8.73
	Dry Summer (s)	0.48	0.57	2.22	0.11	0.78	0.56	4.71
	Dry Winter (w)	0.58	0.24	6.96	0.17	1.14	0.10	9.19
	Subtotal	1.49	1.41	12.51	1.02	5.46	0.75	22.63
Snow (D)	Humid (f)	0.07	0.33	1.17	0.29	1.22	0.01	3.09
	Dry Summer (s)	0.01	0.02	0.58	0.05	0.00	0.11	0.76
	Dry Winter (w)	0.04	0.00	0.87	0.08	0.07	0.15	1.22
	Subtotal	0.12	0.36	2.62	0.42	1.29	0.27	5.07
Polar (E)	Tundra (T)	0.00	0.00	0.00	0.01	0.00	0.00	0.01
	Frost(F)	0.25	0.98	2.26	0.11	0.26	0.32	4.18
	Subtotal	0.25	0.98	2.26	0.12	0.27	0.32	4.19
Total		4.54	10.01	35.86	16.39	28.64	4.57	100.00

and passive margin settings) would be representative of the climate influence and sediment discharge of its largest source catchment (Fig. 21C).

For example, the Mississippi and Ganges/Brahmaputra systems (Fig. 3A and B) are both large but given a similar sized storm cell, the smaller source catchments of the Ganges/Brahmaputra foreland basin may locally influence an entire source catchment while only influencing a small portion of the larger Mississippi source catchment. The influence of a storm cell on the entire source catchment of a localized region in the Ganges/Brahmaputra system suggests a direct sediment discharge response to its terrestrial sink (Fig. 21B). In comparison, the larger source catchment of the Mississippi system may be able buffer a similar sized storm cell before a sediment signal propagation is recorded at the terrestrial sink (Fig. 21C).

### 4.4. Source catchment influence on the terrestrial sink

The terrestrial sink is of particular importance because it marks the first zone of sediment sequestration and potential preservation in the stratigraphic record (Fig. 22). Furthermore, the terrestrial sink is often understated even though it plays a vital role in understanding the dynamics of sedimentary delivery to the marine environment (see Castelltort and Van Den Driessche, 2003, Simpson and Castelltort, 2012; Romans et al., 2016).

The character of a sediment signal propagation will depend on the transfer efficiency and the perturbation of the sediment supply. Allen (2008) termed a sediment signal response at a terrestrial sink that is able to respond to perturbations in sediment supply as a system in a steady state. Otherwise the system enters a reactive, buffered or transient state that will influence the cumulative and temporal response of sediment discharge downstream. Ultimately, sediment signal propagation will depend on the timescales of tectonic and climatic perturbations influencing sediment discharge and the capacity of a system to response to those changes (Blum and Hattier-Womack, 2009; Romans et al., 2016).

It is not our intention here to review each type of sediment signal propagation (see Romans et al., 2016 and references therein), but rather to discuss the likely overarching influence source catchment morphology has on sediment signal propagation into the terrestrial sink. A large terrestrial sink fed by smaller but all significantly contributing source catchments may receive a different sediment discharge signal from different contributing source catchment characteristics because of variations in their morphology, climate, outlet spacing and lithology (Figs. 21A, B, and 22A). In addition, each source catchment may have different perturbations of sediment discharge and a different response time to that sediment supply input. The variability in sediment discharge and repeat-response times of each contributing source catchment will interfere with one another downstream of the terrestrial sink (Fig. 22B). This type of response would be characteristic of a foreland, extensional, strike-slip or intracratonic tectonic regime.

A small terrestrial sink fed by one large source catchment would have a sediment discharge and a sediment signal propagation that is representative of that one source catchment characteristic (e.g., morphology, climate, lithology, tectonics; Fig. 21C). Any sediment signal propagation change is representative of the sediment discharge and perturbations controls of its largest contributing source catchment (Fig. 22A). As such, it may be easier to infer changes in perturbations and/or sediment discharge volumes in systems fed by one large source catchment rather than an amalgamation of multiple source catchments. This response type would be characteristic of a passive margin or forearc setting.

The scale of the terrestrial sink and transport zone will influence sediment signal propagation downstream by increasing potential sediment signal shredding with increasing transport distance (Castelltort and Van Den Driessche, 2003; Jerolmack and Paola, 2010; Romans et al., 2016). Large passive margins and foreland settings with a large absolute
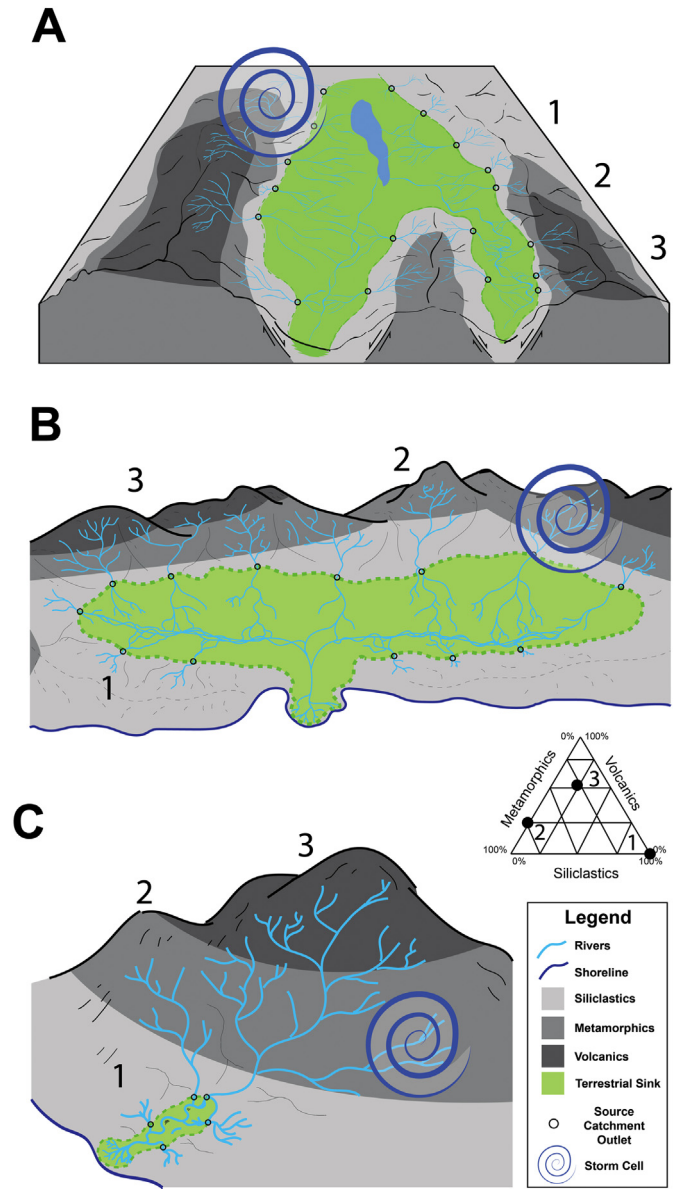
Fig. 21. Schematic illustration of the morphology of source catchment contributions to terrestrial sinks by tectonic regime. (A) Typical catchment configuration of intracratonic, strike-slip or extensional tectonic regimes consisting of numerous smaller source catchments contributing to a relatively large terrestrial sink with a low source-to-sink relief change. (B) Typical foreland basin that consists of numerous smaller source catchments draining through a relatively mid-sized terrestrial sink and a medium source-to-sink relief change. (C) Typical forearc or passive margin configuration consisting of few larger source catchments draining through a relatively small terrestrial sink and a medium to high source-to-sink relief change. The ternary diagram shows the proportion of siliciclastics, metamorphics and volcanics for specific source catchments 1, 2 and 3 (modified after Weltje, 2012). See text for discussion. Note the illustration is shown without scale and relates the terrestrial sink area relative to its total catchment size.

terrestrial sink area will thus have a large area to diffuse a sediment signal in comparison to smaller systems of extensional, strike-slip and forearc settings. However, it is important to reiterate that while passive margins typically have a large terrestrial sink component, the terrestrial sink is small relative to its total catchment area in comparison to a foreland setting. A larger transport zone of sediments from source to terrestrial sink in passive margins will likely decrease both water and sediment discharge first recorded in the terrestrial sink (Fig. 22B). A decrease in water discharge may be especially important for millennial scale perturbations by reducing the amount of water that is able to remobilize sediments stored in the terrestrial sink.

Source catchment characteristics influencing sediment discharge will influence grain size distributions of the terrestrial sink. For instance, an increase in initial sediment discharge decreases the rate of initial grain size fining (Duller et al., 2010). Tectonic uplift in the source catchment will initially increase grain size at the proximal fan while increased precipitation will increase in the lateral extent of a coarse grained fan (Armitage et al., 2011). This is particularly relevant to extensional, strike-slip and foreland tectonic settings where the terrestrial sink is typically bounded by numerous but smaller high relief source catchment regions. The use of grain size in defining spatial trends, sediment supply characteristics and controls on fluvial successions over different spatial and temporal scales (Duller et al., 2010) is thereby complicated by the along strike variability observed in sediment discharge of the contributing source catchments. Grain size profiles in these systems may then represent a lateral coalescence of variability in source catchment discharge that contribute over different spatial and temporal scales. Large mature passive margins that are represented by a few but large source catchments with a large low-gradient transfer zone before their terrestrial sink would potentially show less spatial and temporal variability in grain size (Fig. 22B). Forearc and young passive

margins settings would similarly show a reduced along-strike variability in grain size from fewer significant source catchments. However, the temporal change in grain size profiles may be more dramatic than a large passive margin because there is less low-gradient area to buffer any change in boundary conditions of its source catchment.

4.5. Terrestrial sink influence on the source to sink system

The influence of source catchment morphology on sediment discharge, grain size distributions, sediment composition and a range in source-derived perturbations in sediment discharge to the terrestrial sink, will have a broader influence on the source-to-sink system (see Helland-Hansen et al., 2016). A change in sediment discharge and composition at the marine sink may reflect a change in source catchment controls on the terrestrial sink. This may represent the entire source catchment area or a regional influence on only a few or a single source catchment (Fig. 22A). For instance, sediment budgets of the Indus system are an exceptional example showing that since the last glacial maximum, approximately 31–40% of the total sediment stored on its continental shelf is explained by the release of sediments from the
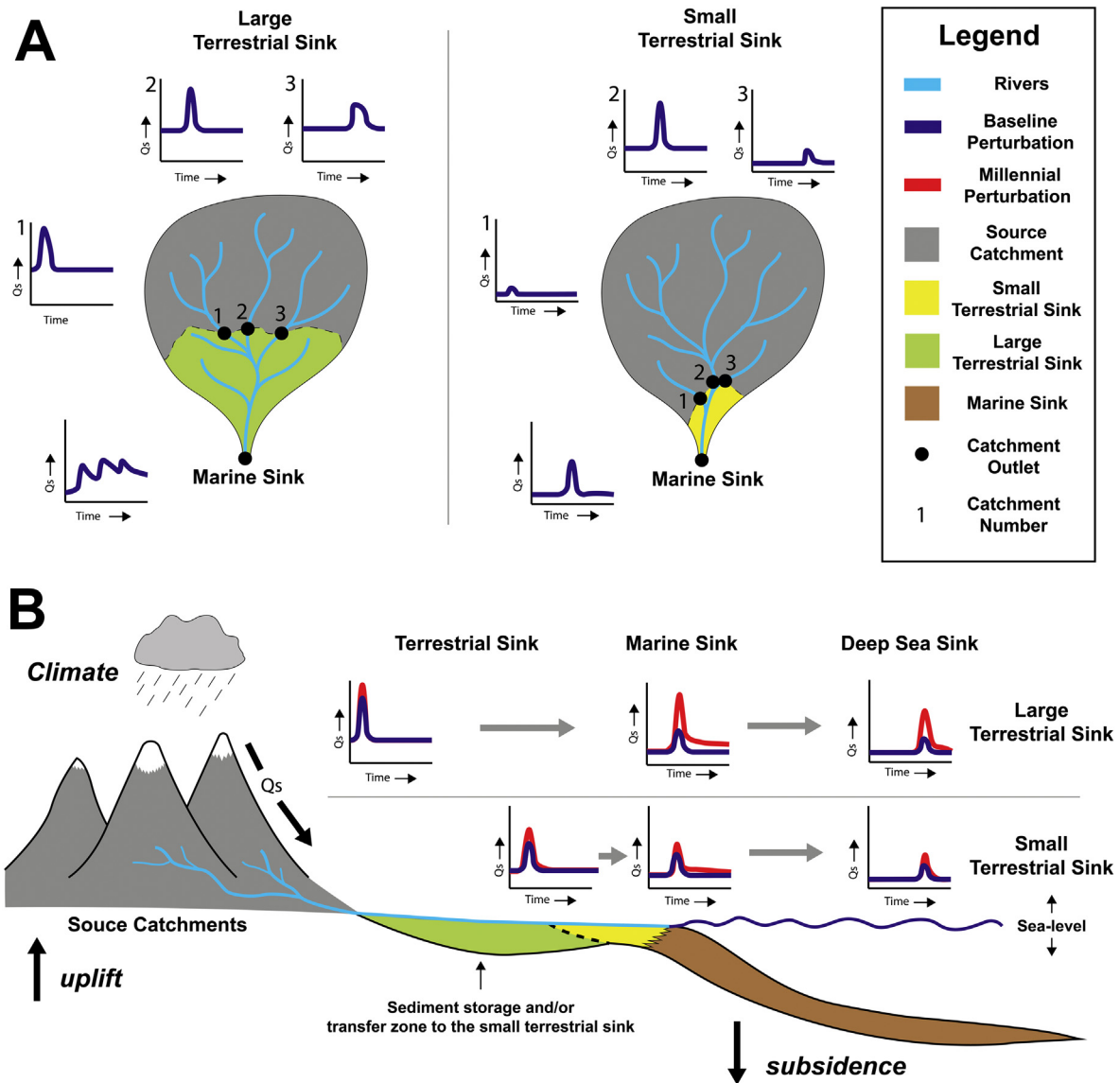
Fig. 22. (A) shows the sediment signal propagation along the strike of a large terrestrial sink (e.g., foreland setting) and a small terrestrial sink (e.g., passive margin) for a similar sized S2S system. (B) shows the sediment signal propagation along the dip of the same system for a large and small terrestrial sink for a baseline and a millennial sediment discharge perturbation. See text for discussion. Part B is modified after Castelltort and Van Den Driessche (2003) and Romans et al. (2016).

Naga Parbat region that accounts for only 5% of the mountainous source catchment (Clift and Giosan, 2014).

Sediment discharge variability at the marine sink increases with decreasing catchment size (Wood et al., 1990; Singh, 1997; Meybeck et al., 2003). For instance, the Santa Ana River in southern California is a good example of a small S2S system with a small terrestrial sink where climatic signals in the source catchment are directly transmitted to sedimentation in the deep-sea sink (Covault et al., 2010). In contrast, a large low gradient region and/or terrestrial sink (e.g., large mature passive margins and foreland settings) will increase sediment signal shredding (Jerolmack and Paola, 2010) and decrease the potential to transfer a source-derived sediment signal to the marine sink. In fact, Castelltort and Van Den Driessche (2003) calculated a transport zone (including its terrestrial sink) >300 km can diffuse even millenial scale pertubations before sedimentation occurs at the marine realm. Furthermore, sea level fluctuations will introduce variability by not only remobilizing floodplain deposits but causing upstream catchment denudation as the fluvial system responds to base level change (Schumm, 1993; Bentley et al., 2016) and fluvial systems potentially extend basinward, reaching the shelf edge and causing sediment bypass to the basin floor (see Shanmugam, 2016). The Indus (Clift and Giosan, 2014), Ganges/Bahramputra (Goodbred and Kuehl, 1999) and Missisippi River basins (Bentley et al., 2016) are examples where changes to deep water deposition have been attributed to sea-level flucations as opposed to changes affecting sediment discharge from source catchment change (Shanmugam et al., 2015; Romans et al., 2016).

While source catchment sediment signal propagation is reduced and potentially destroyed completely in the terrestrial sink of passive margins and foreland settings, the characteristics of the terrestrial sink may have a long-term geological influence on marine sedimentation. As the preserved stratigraphy is composed of an incomplete record of infrequent but large magnitude events (Leeder et al., 1998; Corbett et al., 2014; Miall, 2014), the composition of sediments stored in the terrestrial sink can remobilize during larger millennial episodes that influence the entire system. Simpson and Castelltort (2012) showed numerical models indicating that while the terrestrial sink (>300 km) has the potential to diffuse millennial scale episodes (e.g., Castelltort and Van Den Driessche, 2003), an increase in sedimentation can occur at the marine environment due to an increase in water discharge remobilizing previously stored sediments.

Two similar sized systems, a foreland basin with a large terrestrial sink at the base of an orogeny and a passive margin with a small terrestrial sink but a large transport zone, will likely influence sedimentation differently. During a regular flood episode, both systems can dampen a sediment discharge signal to a similar magnitude at its marine sink (Fig. 22B). In addition, a millennial scale perturbation (tectonic or climatic) in source-derived sediment discharge may not necessarily increase the sediment discharge significantly of either system at the marine sink. However, a millennial scale perturbation in increased water discharge will likely increase sediment remobilization of stored terrestrial sink sediments (Simpson and Castelltort, 2012). A foreland setting with a large terrestrial sink will have a large surface area for the increased water discharge to remobilize sediment downstream. In comparison, a passive margin with a small terrestrial sink system and a large transport zone may not only have less sediment to remobilize but an increase in water discharge may be reduced before any sediments have a chance to be remobilized from the terrestrial sink (Fig. 20A and B).

4.6. Terrestrial sink sediment budgets

Milliman and Syvitski (1992) suggested that if subsidence rates in the foreland Bengal basin were as high as 1–2 cm/yr, 40–80% of the Ganges/Brahmaputra sediment load could be sequestered in its subaerial delta. These are reasonable numbers when compared to recent subsidence rates recorded around the region (Brown and Nicholls, 2015) and may explain the actively accreting and eroding shoreline but limited net land gain over the past two decades (Sarwar and Woodroffe, 2013). In fact, Goodbred and Kuehl (1999) calculated that 30% of the Ganges/Brahmaputra sediment load is stored in floodplains downstream of gauging stations that are typically used to model sediment flux to the Bay of Bengal. A 30% reduction in sediment discharge to the ocean from the Ganges/Brahmaputra River would result in a 1–3% reduction in global sediment budgets, highlighting the importance of terrestrial sinks to global sediment budgets.

Similarly, current empirical models used to predict the global total suspended sediment load are typically constrained by sediment budgets at the oceans (Milliman and Meade, 1983; Milliman and Syvitski, 1992; Ludwig and Probst, 1998; Syvitski and Morehead, 1999; Syvitski and Milliman, 2007) and do not consider the sediment that is lost in the terrestrial sink. Studies in the Amazon basin suggest that approximately half of sediment load of the Amazon is lost in the terrestrial sink (Aalto et al., 2006). While numerical models have started to bridge the gap (e.g., WBMsed; Cohen et al., 2013), the models are often limited by a lack of intra-basinal gauging stations, thereby extrapolating empirical observations from well documented systems (e.g., Mississippi) to the global scale. Our current analysis of source catchment contribution to the terrestrial sink is also limited in that it only shows the relative discharge from each source catchment relative to its total catchment area (e.g., Fig. 1).

The controls on total suspended sediment discharge to the ocean (i.e., lithology, water discharge, catchment area, relief and temperature; Syvtiski and Milliman, 2007) are also likely controls influencing the sediment discharge of source catchments to terrestrial sinks. However, morphological differences between source catchments and the total catchment area may change the relative importance of each parameter. For instance, Mueller and Pitlick (2013) noted the importance of lithology rather than relief or climate on the sediment discharge of small intermontane river catchments. In addition, Aalto et al. (2006) stress the importance of lithology and relief on sediment discharge when analyzing larger catchment contributions to the terrestrial sink of the Bolivean foreland basins. Although beyond the scope of this article, the GTSC database (Fig. 2) provides a digital delineation to evaluate the governing controls on sediment discharge to global terrestrial sinks. Such a study could significantly improve and quantify our current understanding on the diffusive nature of the terrestrial sink (e.g., Castelltort and Van Den Driessche, 2003) and its relation to sediment remobilization arising from larger millennial scale perturbations (e.g., Simpson and Castelltort, 2012).

5. Conclusion

A new global terrestrial sink catchment (GTSC) database depicts drainage patterns of large rivers to modern terrestrial sinks. Our contribution here focuses on a geomorphological and sedimentological perspective on source catchments controls influencing sediment discharge to terrestrial sinks and its implications to broader source-to-sink studies. Observations of source catchment morphology, outlet spacing, climate and lithology distributions show results that imply:

1. In relation to the total catchment area; extensional, strike-slip, intracratonic and foreland tectonic regimes are characterized by a relatively large terrestrial sink that is fed by smaller but numerous, densely spaced and wider source catchments. Passive margins and forearc tectonic regimes are typically characterized by few but larger contributing source catchments feeding a relatively small terrestrial sink. It is important to note, however, that the absolute size of the terrestrial sink is typically large for large passive margins and foreland settings.
2. Seasonal dry summer or winter climates are most common in intracratonic (91%), extensional (81%), strike-slip (77%) and foreland

(59%) tectonic regimes, while less common in forearc (45%) and passive margins (41%).

3. Passive margins, intracratonic, foreland and forearc tectonics regimes are all dominated by high proportion of siliclastics (>50%). Metamorphics are more important in passive margins (>15%), carbonates in foreland regimes (33%) and volcanics/plutonics in forearc regimes (12%). Extensional and strike-slip regimes have lower proportions of siliclastics (<35%) and high volcanic (25%) and plutonic lithologies (15%).

4. Foreland, extensional, strike-slip and intracratonic systems characterized by small, numerous and wider source catchments with seasonal climates and varied lithologies will increase along-strike variability in sediment discharge to their terrestrial sinks. Passive margins and forearc characterized by few but large source catchments with less seasonal climates and less variance in lithology will decrease along-strike variability in sediment discharge to their terrestrial sinks.

5. Along strike variability in sediment discharge can mix and increase destruction of sediment signal propagation downstream as each source catchment will have different sediment discharge perturbations and response times. Foreland, extensional, strike-slip and intracratonic settings will thus have a greater shredding of individual source catchment sediment signal propagations in their terrestrial sinks in contrast to passive margins and forearc settings.

6. On longer geological timescales that form a source-to-sink perspective, millennial scale perturbations in sediment discharge that dominate the stratigraphic record are influenced by the remobilization of previously stored sediments from the terrestrial to marine sink. Source catchment morphology, climate and lithology influencing sediment discharge and composition of the terrestrial sink may thus influence the longer term preservation of marine sedimentary successions.

The GTSC database highlights the controls on the terrestrial sink, its influence on the broader sediment routing system, yet our quantitative knowledge in understanding the relationships between the two is limited. In fact, global denudation rates and the sequestration of sediment in terrestrial sinks over various temporal and spatial scales remain a large unknown. This contribution provides but one small piece towards the objective to understand and quantify the controls on sedimentary budgets of source-to-sink systems.

Appendix A

The contribution of exorheic catchments draining to a body of water in ascending order based on its contribution to the total exorheic area. The data shows the number of catchments, percentage that those are source catchments, total catchment area, percentage of the total exorheic area, percentage of the total catchment area that is a terrestrial sink and the distribution of catchments draining to epicontinental, narrow shelves or wide shelves.

Body of water	Number of catchments	% source catchments	Total catchment area (km^2)	% of total exorheic area	% of catchment area as terrestrial sink	% epicontinental seaway	% narrow cont. shelves (<75 km)	% wide cont. shelves (>75 km)
South Atlantic Ocean	13,449	74.7	15,732,896	15.78	10.0	0.0	47.2	52.8
Kara Sea	9531	62.5	6,926,092	6.95	3.8	96.4	1.0	2.6
Gulf of Mexico	4390	62.1	4,960,852	4.98	8.7	0.0	71.9	28.1
North Atlantic Ocean	7631	69.7	4,163,361	4.18	15.3	0.0	60.8	39.2
Laptev Sea	2037	76.4	3,696,963	3.71	0.7	0.0	0.9	99.1
Gulf of Guinea	4021	67.9	3,438,739	3.45	15.0	0.0	95.2	4.8
Mediterranean Sea - Eastern Basin	7529	72.2	3,431,506	3.44	24.9	0.0	98.3	1.7
Indian Ocean	5472	71.6	3,234,878	3.24	14.5	1.2	79.9	18.9
Hudson Bay	1132	100.0	3,128,343	3.14	0.0	100.0	0.0	0.0
Rio de La Plata	2333	74.9	3,092,018	3.10	41.3	0.0	0.0	100.0
Bay of Bengal	3534	68.6	2,895,903	2.90	26.5	0.0	36.2	63.8
Mozambique Channel	3576	72.7	2,761,742	2.77	15.0	0.0	45.6	54.4
Sea of Okhotsk	7262	87.3	2,688,999	2.70	14.5	99.7	0.3	0.0
South China Sea	4049	70.0	2,364,409	2.37	12.7	99.7	0.3	0.0
Eastern China Sea	2753	81.7	2,134,875	2.14	13.3	100.0	0.0	0.0
Beaufort Sea	1072	59.7	2,055,886	2.06	2.8	0.0	13.1	86.8
North Pacific Ocean	4927	83.3	1,928,001	1.93	6.0	0.6	62.1	37.4
Arabian Sea	2691	72.7	1,788,898	1.79	37.3	1.0	10.9	88.1
Black Sea	3228	75.2	1,779,842	1.78	13.7	100.0	0.0	0.0
Yellow Sea	3561	79.3	1,662,074	1.67	25.2	100.0	0.0	0.0
Bering Sea	8284	67.6	1,619,480	1.62	12.5	92.1	6.6	1.3
Gulf of St. Lawrence	1008	100.0	1,547,605	1.55	0.0	98.2	0.2	1.6
The Northwestern Passages	5191	98.6	1,442,068	1.45	0.1	95.5	4.5	0.0
East Siberian Sea	3381	64,6	1,313,518	1.32	11.6	50.0	0.1	50.0
South Pacific Ocean	4958	91.5	1,264,867	1.27	5.4	0.9	79.1	19.9
Persian Gulf	2565	59.5	1,196,389	1.20	25.0	99.5	0.5	0.0
Great Australian Bight	2239	80.0	1,080,674	1.08	45.6	0.0	10.3	89.7
Caribbean Sea	3909	71.5	1,037,343	1.04	20.9	0.0	76.4	23.6
Gulf of California	2451	66.0	958,019	0.96	17.5	0.0	31.6	68.4
Arafura Sea	2033	64.5	861,951	0.86	38.9	100.0	0.0	0.0
Andaman or Burma Sea	1162	77.6	780,660	0.78	10.2	98.3	1.7	0.0

Appendix A (*continued*)

Body of water	Number of catchments	% source catchments	Total catchment area (km^2)	% of total exorheic area	% of catchment area as terrestrial sink	% epicontinental seaway	% narrow cont. shelves (<75 km)	% wide cont. shelves (>75 km)
Coral Sea	1665	75.8	700,992	0.70	5.8	1.1	22.4	76.5
White Sea	596	85.9	656,752	0.00	1.3	99.5	0.0	0.5
North Sea	1429	72.8	606,309	0.61	14.5	41.9	3.6	54.6
Sea of Azov	782	52.0	587,704	0.59	12.4	100.0	0.0	0.0
Barents Sea	1160	89.5	583,442	0.59	2.0	66.7	2.8	30.5
Baltic Sea	1554	70.1	569,129	0.57	9.0	100.0	0.0	0.0
The Coastal Waters of Southeast Alaska and British Columbia	1655	99.0	564,608	0.57	0.2	0.0	6.5	93.5
Red Sea	2275	60.4	523,428	0.52	16.6	100.0	0.0	0.0
Gulf of Finland	146	100.0	505,421	0.51	0.0	100.0	0.0	0.0
Gulf of Bothnia	306	100.0	481,267	0.00	0.0	100.0	0.0	0.0
Hudson Strait	586	100.0	413,503	0.41	0.0	13.6	0.2	86.2
Timor Sea	1002	70.6	349,945	0.35	15.7	100.0	0.0	0.0
Japan Sea	1260	94.4	341,776	0.34	1.6	100.0	0.0	0.0
Gulf of Thailand	1056	73.4	323,427	0.32	31.0	100.0	0.0	0.0
Mediterranean Sea - Western Basin	747	83.1	314,450	0.32	4.4	0.0	100.0	0.0
Java Sea	1130	63.4	308,662	0.31	26.9	96.5	3.5	0.0
Labrador Sea	760	100.0	289,426	0.29	0.0	0.0	33.7	66.3
Bay of Biscay	343	84.5	282,395	0.28	1.9	0.0	15.4	84.6
Gulf of Alaska	1009	87.6	241,193	0.24	3.1	39.9	58.0	2.2
Tasman Sea	813	92.7	238,251	0.24	2.0	0.0	87.6	12.4
Adriatic Sea	861	82.2	230,989	0.23	16.8	0.0	71.1	28.9
Aegean Sea	1118	93.5	214,308	0.21	5.8	26.2	56.2	17.6
Chukchi Sea	994	68.2	199,973	0.20	10.2	77.7	1.3	21.0
Gulf of Aden	811	68.3	198,329	0.20	9.1	1.4	98.6	0.0
Philippine Sea	1309	92.4	175,908	0.18	2.5	45.8	53.6	0.6
Malacca Strait	839	65.9	169,472	0.17	15.9	100.0	0.0	0.0
Makassar Strait	618	82.5	163,003	0.16	8.5	100.0	0.0	0.0
Celebes Sea	512	88.7	144,621	0.15	2.6	99.9	0.1	0.0
Balearic (Iberian Sea)	209	90.0	136,556	0.14	1.9	0.0	100.0	0.0
Bismarck Sea	392	87.0	133,162	0.13	4.2	95.3	4.7	0.0
English Channel	267	95.1	127,276	0.13	0.5	99.1	0.0	0.9
Gulf of Oman	457	66.3	115,964	0.12	8.9	0.0	100.0	0.0
Laccadive Sea	322	75.5	107,914	0.11	19.6	0.0	84.9	15.1
Norwegian Sea	759	100.0	106,681	0.11	0.0	0.0	67.7	32.3
Davis Strait	629	100.0	105,859	0.11	0.0	0.2	63.6	36.2
Skagerrak	113	100.0	99,548	0.10	0.0	0.0	98.7	1.3
Baffin Bay	578	100.0	99,274	0.10	0.0	11.2	88.8	0.0
Kattegat	271	100.0	93,418	0.09	0.0	41.5	2.8	55.6
Bass Strait	361	83.4	91,889	0.09	4.1	0.0	36.5	63.5
Alboran Sea	250	83.2	88,113	0.09	11.9	0.0	100.0	0.0
Solomon Sea	559	98.9	86,237	0.09	0.5	3.9	94.5	1.6
Tyrrhenian Sea	420	90.2	84,460	0.08	4.0	0.0	100.0	0.0
Bay of Fundy	118	100.0	80,739	0.08	0.0	99.6	0.0	0.4
Sulu Sea	478	84.7	69,252	0.07	5.0	100.0	0.0	0.0
Greenland Sea	373	100.0	65,269	0.07	0.0	0.0	100.0	0.0
Banda Sea	513	97.9	64,082	0.06	0.2	100.0	0.0	0.0
Ceram Sea	292	87.7	62,240	0.06	5.5	92.8	7.2	0.0
Gulf of Riga	83	100.0	62,219	0.06	0.0	100.0	0.0	0.0
Ionian Sea	429	91.1	58,748	0.06	2.2	0.0	94.6	5.4
Irish Sea and St. George's Channel	207	100.0	39,234	0.04	0.0	100.0	0.0	0.0
Sea of Marmara	120	95.8	39,027	0.04	2.0	92.8	7.2	0.0
Seto Naikai or Inland Sea	206	93.2	38,739	0.04	2.0	98.0	1.2	0.8
Arctic Ocean	206	100.0	34,437	0.03	0.0	6.1	93.9	0.0
Gulf of Suez	142	93.0	33,755	0.03	0.9	100.0	0.0	0.0
Gulf of Boni	204	82.4	32,965	0.03	10.8	100.0	0.0	0.0
Inner Seas off the West Coast of Scotland	333	100.0	31,392	0.03	0.0	6.2	3.0	90.8
Bristol Channel	60	100.0	29,007	0.03	0.0	0.0	0.0	100.0
Gulf of Tomini	163	96.9	28,072	0.03	1.0	100.0	0.0	0.0
Celtic Sea	106	100.0	21,890	0.02	0.0	2.1	1.2	96.7
Savu Sea	196	100.0	18,554	0.02	0.0	100.0	0.0	0.0
Gulf of Aqaba	64	100.0	17,873	0.02	0.0	100.0	0.0	0.0
Flores Sea	145	100.0	13,620	0.01	0.0	100.0	0.0	0.0
Halmahera Sea	124	100.0	13,000	0.01	0.0	100.0	0.0	0.0
Bali Sea	139	100.0	10,185	0.01	0.0	96.4	3.6	0.0
Molukka Sea	160	100.0	9255	0.01	0.0	99.0	1.0	0.0
Lincoln Sea	40	100.0	5992	0.01	0.0	0.0	100.0	0.0
Singapore Strait	29	100.0	3731	0.00	0.0	100.0	0.0	0.0
Ligurian Sea	41	100.0	3208	0.00	0.0	0.0	100.0	0.0
Strait of Gibraltar	18	100.0	2471	0.00	0.0	0.0	100.0	0.0
Total/average	169,271	85.1	99,712,836	100	7.9	49.9	30.0	20.1

Appendix B

A summary of first- and second-order climate distribution for global catchments and source catchments according to the Köppen-Geiger (Kottek, 2006) classification scheme.

Climate	Humid (f)	Monsoon (m)	Dry summer (s)	Dry winter (w)	Tundra (T)	Frost (F)	Total
Global catchments							
Equatorial (A)	4.85	3.77	0.56	12.99	N/A	N/A	22.16
Arid (B)	N/A	N/A	12.58	18.50	N/A	N/A	31.09
Warm temperate (C)	8.80	N/A	2.85	4.41	N/A	N/A	16.06
Snow (D)	20.78	N/A	0.84	3.61	N/A	N/A	25.23
Polar (E)	N/A	N/A	N/A	N/A	5.43	0.04	5.47
Total	34.40	3.80	16.80	39.50	5.40	0.04	100.00
Source catchments							
Equatorial (A)	5.40	4.02	0.57	13.25	N/A	N/A	23.24
Arid (B)	N/A	N/A	10.90	13.46	N/A	N/A	24.36
Warm temperate (C)	8.85	N/A	3.15	4.37	N/A	N/A	16.38
Snow (D)	24.64	N/A	0.98	3.91	N/A	N/A	29.52
Polar (E)	N/A	N/A	N/A	N/A	6.46	0.05	6.51
Total	38.8	4.02	15.7	35.1	6.5	0.05	100

Appendix C. Supplementary data

Supplementary data to this article can be found online at https://doi.org/10.1016/j.geomorph.2018.05.007.

References

Aalto, R., Dunne, T., Guyot, J.L., 2006. Geomorphic controls on Andean denudation rates. J. Geol. 114:85–99. https://doi.org/10.1086/498101.

Allen, P.A., 2008. Time scales of tectonic landscapes and their sediment routing systems. Geol. Soc. Lond. Spec. Publ. 296:7–28. https://doi.org/10.1144/SP296.2.

Allmendinger, R.W., Jordan, T.E., Kay, S.M., Isacks, B.L., 1997. The evolution of the Altiplano-Puna Plateau of the Central Andes. Annu. Rev. Earth Planet. Sci. 25: 139–174. https://doi.org/10.1146/annurev.earth.25.1.139.

Armitage, J.J., Duller, R.A., Whittaker, A.C., Allen, P.A., 2011. Transformation of tectonic and climatic signals from source to sedimentary archive. Nat. Geosci. 4:231–235. https://doi.org/10.1038/ngeo1087.

Arribas, J., Tortosa, A., 2003. Detrital modes in sedimenticlastic sands from low-order streams in the Iberian Range, Spain: the potential for sand generation by different sedimentary rocks. Sediment. Geol. 159:275–303. https://doi.org/10.1016/S0037-0738(02)00332-9.

Bentley, S.J., Blum, M.D., Maloney, J., Pond, L., Paulsell, R., 2016. The Mississippi River source-to-sink system: perspectives on tectonic, climatic, and anthropogenic influences, Miocene to Anthropocene. Earth Sci. Rev. 153:139–174. https://doi.org/10.1016/j.earscirev.2015.11.001.

Bierkens, M.F.P., 2015. Global hydrology: 2015: State, trends, and directions. Water Resour. Res. 51:4923–4947. https://doi.org/10.1002/2015WR017173.

Bird, P., 2003. An updated digital model of plate boundaries. Geochem. Geophys. Geosyst. 4:1027. https://doi.org/10.1029/2001GC000252.

Blum, M.D., Hattier-Womack, J., 2009. Climate change, sea-level change, and fluvial sediment supply to deepwater depositional systems. Extern. Control. Deep. Depos. Syst. 92:15–39.

Blum, M.D., Tornqvist, T.E., 2000. Fluvial responses to climate and sea-level change: a review and look forward. Sedimentology 47:2–48.

Brown, S., Nicholls, R.J., 2015. Subsidence and human influences in mega deltas: the case of the Ganges-Brahmaputra-Meghna. Sci. Total Environ. 527–528:362–374. https://doi.org/10.1016/j.scitotenv.2015.04.124.

Castelltort, S., Van Den Driessche, J., 2003. How plausible are high-frequency sediment supply-driven cycles in the stratigraphic record? Sediment. Geol. 157: 3–13. https://doi.org/10.1016/S0037-0738(03)00066-6.

Clift, P.D., Giosan, L., 2014. Sediment fluxes and buffering in the post-glacial Indus Basin. Basin Res. 26:369–386. https://doi.org/10.1111/bre.12038.

Cohen, S., Kettner, A.J., Syvitski, J.P.M., Fekete, B.M., 2013. WBMsed, a distributed global-scale riverine sediment flux model: model description and validation. Comput. Geosci. 53:80–93. https://doi.org/10.1016/j.cageo.2011.08.011.

Corbett, D.R., Walsh, J.P., Harris, C.K., Ogston, A.S., Orpin, A.R., 2014. Formation and preservation of sedimentary strata from coastal events: insights from measurements and modeling. Cont. Shelf Res. 86:1–5. https://doi.org/10.1016/j.csr.2014.06.011.

Covault, J.A., Romans, B.W., Fildani, A., McGann, M., Graham, S.A., 2010. Rapid climatic signal propagation from source to sink in a southern California sediment-routing system. J. Geol. 118:247–259. https://doi.org/10.1086/651539.

Cunningham, D., 2010. Tectonic setting and structural evolution of the Late Cenozoic Gobi Altai orogen. Geol. Soc. Lond. Spec. Publ. 338:361–387.

[dataset] Danielson, J.J., Gesch, D.B., 2011. Global multi-resolution terrain elevation data 2010 (GMTED2010). U.S. Geol. Surv. Open File Rep. 26 (2011-1073).

D'Arcy, M., Whittaker, A.C., 2014. Geomorphic constraints on landscape sensitivity to climate in tectonically active areas. Geomorphology 204:366–381. https://doi.org/10.1016/j.geomorph.2013.08.019.

Davidson, S.K., Hartley, A.J., Weissmann, G.S., Nichols, G.J., Scuderi, L.A., 2013. Geomorphic elements on modern distributive fluvial systems. Geomorphology 180–181:82–95. https://doi.org/10.1016/j.geomorph.2012.09.008.

DeCelles, P.G., Cavazza, W., 1999. A comparison of fluvial megafans in the Cordilleran (Upper Cretaceous) and modern Himalayan foreland basin systems. Bull. Geol. Soc. Am. 111: 1315–1334. https://doi.org/10.1130/0016-7606(1999)111<1315:ACOFMI>2.3.CO;2.

Decelles, P.G., Giles, K.A., 1996. Foreland basin systems. Basin Res. 8:105–123.

DeCelles, P.G., Carrapa, B., Horton, B.K., Gehrels, G.E., 2011. Cenozoic foreland basin system in the central Andes of northwestern Argentina: implications for Andean geodynamics and modes of deformation. Tectonics 30, TC6013. https://doi.org/10.1029/2011TC002948.

Dewey, J.F., Hempton, M.R., Kidd, W.S.F., Saroglu, F., Şengör, A.M.C., 1986. Shortening of continental lithosphere: the neotectonics of eastern Anatolia—a young collision zone. Geol. Soc. Lond. Spec. Publ. 19:1–36.

Döll, P., Lehner, B., 2002. Validation of a new global 30-min drainage direction map. J. Hydrol. 258:214–231. https://doi.org/10.1016/S0022-1694(01)00565-0.

Duller, R.A., Whittaker, A.C., Fedele, J.J., Whitchurch, A.L., Springett, J., Smithells, R., Fordyce, S., Allen, P.A., 2010. From grain size to tectonics. J. Geophys. Res. 115, F03022. https://doi.org/10.1029/2009JF001495.

Dürr, H., Laruelle, G., Kempen, C., Slomp, C., Meybeck, M., Middelkoop, H., 2011. Worldwide typology of nearshore coastal systems: defining the estuarine filter of river inputs to the oceans. Estuar. Coasts 34:441–458. https://doi.org/10.1007/s12237-011-9381-y.

ESRI, 2017. ESRI (Environmental Systems Resource Institute). 2017. ArcMap 10.3.1, Redlands, California.

Getirana, A.C.V., Boone, A., Yamazaki, D., Decharme, B., Papa, F., Mognard, N., 2012. The hydrological modeling and analysis platform (HyMAP): evaluation in the Amazon Basin. J. Hydrometeorol. 13:1641–1665. https://doi.org/10.1175/JHM-D-12-021.1.

Goodbred, S.L., Kuehl, S.A., 1999. Holocene and modern sediment budgets for the Ganges-Brahmaputra river system: evidence for highstand dispersal to flood-plain, shelf, and deep-sea depocenters. Geology 27:559–562. https://doi.org/10.1130/0091-7613(1999)027<0559:HAMSBF>2.3.CO;2.

Hack, J.T., 1957. Studies of longitudinal stream profiles in Virginia and Maryland. US Geol. Surv. Prof. Pap. 45–97 294-B.

Harris, P.T., Macmillan-Lawler, M., Rupp, J., Baker, E.K., 2014. Geomorphology of the oceans. Mar. Geol. 352:4–24. https://doi.org/10.1016/j.margeo.2014.01.011.

Hartley, A.J., Weissmann, G.S., Nichols, G.J., Warwick, G., 2010. Large distributive fluvial systems: characteristics, distribution, and controls on development. J. Sediment. Res. 80:167–183. https://doi.org/10.2110/jsr.2010.016.

Hartmann, J., Moosdorf, N., 2012. The new global lithological map database GLiM: a representation of rock properties at the Earth surface. Geochem. Geophys. Geosyst. 13, Q12004. https://doi.org/10.1029/2012GC004370.

Helland-Hansen, W., Sømme, T.O., Martinsen, O.J., Lunt, I., Thurmond, J., 2016. Deciphering Earth's natural hourglasses: perspectives on source-to-sink analysis. J. Sediment. Res. 86:1008–1033. https://doi.org/10.2110/jsr.2016.56.

Honthaas, C., Réhault, J.-P., Maury, R.C., Bellon, H., Hémond, C., Malod, J.-A., Cornée, J.-J., Villeneuve, M., Cotten, J., Burhanuddin, S., Guillou, H., Arnaud, N., 1998. A Neogene back-arc origin for the Banda Sea basins: geochemical and geochronological constraints from the Banda ridges (East Indonesia). Tectonophysics 298:297–317. https://doi.org/10.1016/S0040-1951(98)00190-5.

Hovius, N., 1996. Regular spacing of drainage outlets from linear mountain belts. Basin Res. 8:29–44. https://doi.org/10.1111/j.1365-2117.1996.tb00113.x.

Ingersoll, R.V., 2012. Tectonics of sedimentary basins, with revised nomenclature. In: Busby, C., Azor, A. (Eds.), Tectonics of Sedimentary Basins Recent Advances. Wiley-Blackwell Publishing Ltd, Chichester, West Sussex.

Jerolmack, D.J., Paola, C., 2010. Shredding of environmental signals by sediment transport. Geophys. Res. Lett. 37:1–5. https://doi.org/10.1029/2010GL044638.

Jervey, M.T., 1988. Quantitative geological modeling of siliciclastic rock sequences and their seismic expression. Sea-Level Chang. 42:47–69.

[dataset] Kottek, M., 2006. World map of the Köppen-Giger climate classification updated. Meteorol. Z. 15:259–263.

Laruelle, G.G., Dürr, H.H., Lauerwald, R., Hartmann, J., Slomp, C.P., Goossens, N., Regnier, P.A.G., 2013. Global multi-scale segmentation of continental and coastal waters from the watersheds to the continental margins. Hydrol. Earth Syst. Sci. 17: 2029–2051. https://doi.org/10.5194/hess-17-2029-2013.

Leeder, M.R. Harris, T., Kirkby, M.J., Hovius, N., Leeder, M., 1998. Sediment supply and climate change; implications for basin stratigraphy\nBasin research; thematic set on sediment supply to basins. Basin Res. 10:7–18. https://doi.org/10.1046/j.1365-2117.1998.00054.x.

Lehner, B., Verdin, K., Jarvis, A., 2008. New global hydrography derived from spaceborne elevation data. EOS Trans. Am. Geophys. Union 89:93–94. https://doi.org/10.1029/2008EO100001.

Leier, A.L., DeCelles, P.G., Pelletier, J.D., 2005. Mountains, monsoons, and megafans. Geology 33:289–292. https://doi.org/10.1130/G21228.1.

Ludwig, W., Probst, J.L., 1998. River sediment discharge to the oceans: present-day controls and global budgets. Am. J. Sci. 298:265–295. https://doi.org/10.2475/ajs.298.4.265.

Mann, P., Burke, K., 1984. Neotectonics of the Caribbean. Rev. Geophys. 22:309–362. https://doi.org/10.1029/RG022i004p00309.

Marsaglia, K.M., 1995. Interarc and Backarc Basins. In: Busby, C.J., Ingersoll, R.V (Eds.), Tectonics of Sedimentary Basins. Blackwell Science, Oxford, pp. 299–330.

Meybeck, M., Laroche, L., Dürr, H.H., Syvitski, J.P.M., 2003. Global variability of daily total suspended solids and their fluxes in rivers. Glob. Planet. Chang. 39:65–93. https://doi.org/10.1016/S0921-8181(03)00018-3.

Miall, A., 2014. The emptiness of the stratigraphic record: a preliminary evaluation of missing time in the Mesaverde Group, Book Cliffs, Utah, U.S.A. J. Sediment. Res. 84, 457–469.

Milliman, J.D., Meade, R.H., 1983. World-wide delivery of river sediment to the oceans. J. Geol. 91:1–21. https://doi.org/10.1086/676943.

Milliman, J.D., Syvitski, J.P.M., 1992. Geomorphic/tectonic control of sediment discharge to the ocean: the importance of small mountainous rivers. J. Geol. 100:525–544. https://doi.org/10.2307/30068527.

Mueller, E.R., Pitlick, J., 2013. Sediment supply and channel morphology in mountain river systems: 1. Relative importance of lithology, topography, and climate. J. Geophys. Res. Earth Surf. 118:2325–2342. https://doi.org/10.1002/2013JF002843.

Müller, B., Zoback, M. Lou, Fuchs, K., Mastin, L., Gregersen, S., Pavoni, N., Stephansson, O., Ljunggren, C., 1992. Regional patterns of tectonic stress in Europe. J. Geophys. Res. Solid Earth 97:11783–11803. https://doi.org/10.1029/91JB01096.

[dataset] NASA LP DAAC, 2001. MOD 11 - Land Surface Temperature and Emissivity. NASA Land Processes Distributed Active Archive Center (LP DAAC) USGS/Earth Resources Observation and Science (EROS) Center.

Norton, K.P., von Blanckenburg, F., DiBiase, R., Schlunegger, F., Kubik, P.W., 2011. Cosmogenic 10Be-derived denudation rates of the eastern and southern European alps. Int. J. Earth Sci. 100:1163–1179. https://doi.org/10.1007/s00531-010-0626-y.

Nyberg, B., Howell, J.A., 2015. Is the present the key to the past? A global characterization of modern sedimentary basins. Geology. 43:643–646. https://doi.org/10.1130/G36669.1.

Nyberg, B., Howell, J.A., 2016. Global distribution of modern shallow marine shorelines. implications for exploration and reservoir analogue studies. Mar. Pet. Geol. 71: 83–104. https://doi.org/10.1016/j.marpetgeo.2015.11.025.

Nyberg, B., Buckley, S.J., Howell, J.A., Nanson, R.A., 2015. Geometric attribute and shape characterization of modern depositional elements: a quantitative GIS method for empirical analysis. Comput. Geosci. 82:191–204. https://doi.org/10.1016/j.cageo.2015.06.003.

Owen, A., Ebinghaus, A., Hartley, A.J., Santos, M.G.M., Weissmann, G.S., 2017. Multi-scale classification of fluvial architecture: An example from the Palaeocene–Eocene Bighorn Basin, Wyoming. Sedimentology 64:1572–1596. https://doi.org/10.1111/sed.12364.

Palumbo, L., Hetzel, R., Tao, M., Li, X., 2009. Catchment-wide denudation rates at the margin of NE Tibet from in situ-produced cosmogenic 10Be. Terra Nova 117:130–142. https://doi.org/10.1111/j.1365-3121.2010.00982.x.

Reuter, H.I., Nelson, A., Jarvis, A., 2007. An evaluation of void-filling interpolation methods for SRTM data. Int. J. Geogr. Inf. Sci. 21:983–1008. https://doi.org/10.1080/13658810601169899.

Rigon, R., Rodriguez-iturbe, I., Maritan, A., Giacometti, A., Tarboton, D.G., Rinaldo, A., 1996. On Hack"s Law. Water Resour. Res. 32:3367–3374.

Roe, G.H., 2005. Orographic precipitation. Annu. Rev. Earth Planet. Sci. 33:645–671. https://doi.org/10.1146/annurev.earth.33.092203.122541.

Romans, B.W., Castelltort, S., Covault, J.A., Fildani, A., Walsh, J.P., 2016. Environmental signal propagation in sedimentary systems across timescales. Earth Sci. Rev. 153:7–29. https://doi.org/10.1016/j.earscirev.2015.07.012.

Sarwar, M.G.M., Woodroffe, C.D., 2013. Rates of shoreline change along the coast of Bangladesh. J. Coast. Conserv. 17:515–526. https://doi.org/10.1007/s11852-013-0251-6.

Schumm, S.A., 1993. River response to baselevel change: implications for sequence stratigraphy river response to baselevel change: implications for sequence stratigraphy1. Source J. Geol. 101:279–294. https://doi.org/10.1086/648221.

Shanmugam, G., 2016. Submarine fans: a critical retrospective (1950–2015). J. Palaeogeogr. 5:258–277. https://doi.org/10.1016/j.jop.2016.05.007.

Shanmugam, G., Moiola, R.J., Damuth, J.E., 2015. Eustatic Control of Submarine Fan Development BT - Submarine Fans and Related Turbidite Systems. In: Bouma, A.H., Normark, W.R., Barnes, N.E. (Eds.), Springer New York, New York, NY:pp. 23–28 https://doi.org/10.1007/978-1-4612-5114-9_5.

Simpson, G., Castelltort, S., 2012. Model shows that rivers transmit high-frequency climate cycles to the sedimentary record. Geology 40:1131–1134. https://doi.org/10.1130/G33451.1.

Singh, V.P., 1997. Effect of spatial and temporal variability in rainfall and watershed characteristics on stream flow hydrograph. Hydrol. Process. 11:1649–1669. https://doi.org/10.1002/(SICI)1099-1085(19971015)11:12<1649::AID-HYP495>3.0.CO;2-1.

Sólyom, P.B., Tucker, G.E., 2004. Effect of limited storm duration on landscape evolution, drainage basin geometry, and hydrograph shapes. J. Geophys. Res. 109, F03012. https://doi.org/10.1029/2003JF000032.

Sømme, T.O., Jackson, C.A.L., 2013. Source-to-sink analysis of ancient sedimentary systems using a subsurface case study from the Møre-Trøndelag area of southern Norway: part 2 - sediment dispersal and forcing mechanisms. Basin Res. 25: 512–531. https://doi.org/10.1111/bre.12014.

Sømme, T.O., Helland-hansen, W., Martinsen, O.J., Thurmond, J.B., 2009. Relationships between morphological and sedimentological parameters in source-to-sink systems: a basis for predicting semi-quantitative characteristics in subsurface systems. Basin Res. 21:361–387. https://doi.org/10.1111/j.1365-2117.2009.00397.x.

Syvitski, J.P.M., Milliman, J.D., 2007. Geology, geography, and humans battle for dominance over the delivery of fluvial sediment to the coastal ocean. J. Geol. 115:1–19. https://doi.org/10.1086/509246.

Syvitski, J.P., Morehead, M.D., 1999. Estimating river-sediment discharge to the ocean: application to the eel margin, northern California. Mar. Geol. 154:13–28. https://doi.org/10.1016/S0025-3227(98)00100-5.

Syvitski, J.P.M., Vörösmarty, C.J., Kettner, A.J., Green, P., 2005. Impact of humans on the flux of terrestrial sediment to the global coastal ocean. Science 308:376–380. https://doi.org/10.1126/science.1109454.

Vörösmarty, C.J., Fekete, B.M., Meybeck, M., Lammers, R.B., 2000a. Geomorphometric attributes of the global system of rivers at 30-minute spatial resolution. J. Hydrol. 237:17–39. https://doi.org/10.1016/S0022-1694(00)00282-1.

Vörösmarty, C.J., Fekete, B.M., Meybeck, M., Lammers, R.B., 2000b. Global system of rivers: its role in organizing continental land mass and defining land-to-ocean linkages. Glob. Biogeochem. Cycles 14:599–621. https://doi.org/10.1029/1999GB900092.

Vörösmarty, C.J., Green, P., Salisbury, J., Lammers, R.B., 2003. Global water resources: vulnerability from climate change and population growth. Science 289:284–288. https://doi.org/10.1126/science.289.5477.284.

Wang, E., Xu, F.-Y., Zhou, J.-X., Wan, J., Burchfiel, B.C., 2006. Eastward migration of the Qaidam basin and its implications for Cenozoic evolution of the Altyn Tagh fault and associated river systems. Geol. Soc. Am. 118:349–365. https://doi.org/10.1130/B25778.1.

Watson, M.P., Hayward, A.B., Parkinson, D.N., Zhang, Z.M., 1987. Plate tectonic history, basin development and petroleum source rock deposition onshore China. Mar. Pet. Geol. 4:205–225. https://doi.org/10.1016/0264-8172(87)90045-6.

Weissmann, G., Hartley, A., Nichols, G., Scuderi, L., Olson, M., Buehler, H., Banteah, R., 2010. Fluvial form in modern continental sedimentary basins: distributive fluvial systems. Geol. Soc. Am. 38:39–42. https://doi.org/10.1130/G30242.1.

Weissmann, G.S., Hartley, A.J., Scuderi, L.A., Nichols, G.J., Owen, A., Wright, S., Felicia, A.L., Holland, F., Anaya, F.M.L., 2015. Fluvial geomorphic elements in modern sedimentary basins and their potential preservation in the rock record: a review. Geomorphology 250:187–219. https://doi.org/10.1016/j.geomorph.2015.09.005.

Weltje, G.J., 2012. Quantitative models of sediment generation and provenance: state of the art and future developments. Sediment. Geol. 280:4–20. https://doi.org/10.1016/j.sedgeo.2012.03.010.

Wisser, D., Fekete, B.M., Vörösmarty, C.J., Schumann, A.H., 2010. Reconstructing 20th century global hydrography: a contribution to the Global Terrestrial Network- Hydrology (GTN-H). Hydrol. Earth Syst. Sci. 14:1–24. https://doi.org/10.5194/hess-14-1-2010.

Wood, E.F., Sivapalan, M., Beven, K., 1990. Similarity and scale in catchment storm response. Rev. Geophys. https://doi.org/10.1029/RG028i001p00001.

Wulf, H., Bookhagen, B., Scherler, D., 2010. Seasonal precipitation gradients and their impact on fluvial sediment flux in the Northwest Himalaya. Geomorphology 118:13–21. https://doi.org/10.1016/j.geomorph.2009.12.003.

Yi, S., Yi, S., Batten, D.J., Yun, H., Park, S., 2003. Cretaceous and Cenozoic non-marine deposits of the Northern South Yellow Sea Basin, offshore western Korea: palynostratigraphy and palaeoenvironments. Palaeogeogr. Palaeoclimatol. Palaeoecol. 191:15–44. https://doi.org/10.1016/S0031-0182(02)00637-5.

Yueqiao, Z., Yinsheng, M., Nong, Y., Wei, S., Shuwen, D., 2003. Cenozoic extensional stress evolution in North China. J. Geodyn. 36:591–613. https://doi.org/10.1016/j.jog.2003.08.001.

Zoback, M.L., 1992. First- and second-order patterns of stress in the lithosphere: the world stress map project. J. Geophys. Res. Solid Earth 97:11703–11728. https://doi.org/10.1029/92JB00132.